Tectonics®

RESEARCH ARTICLE
10.1029/2025TC008896

Cenozoic Evolution of the North-Eastern Mediterranean Basins

Bertone Nicolò[1,2], Bonini Lorenzo[2,3], Del Ben Anna[2], Brancatelli Giuseppe[4], Camerlenghi Angelo[4], Forlin Edy[4], and Pini Gian Andrea[2]

[1]Department of Civil, Chemical, Environmental, and Material Engineering, University of Bologna, Bologna, Italy, [2]Department of Mathematics, Informatics and Geosciences, University of Trieste, Trieste, Italy, [3]National Institute of Geophysics and Volcanology (INGV), Rome, Italy, [4]National Institute of Oceanography and Applied Geophysics (OGS), Trieste, Italy

Abstract The Eastern Mediterranean lies at the junction of the African, Arabian, and Eurasian plates, a region shaped by a long and complex tectonic history. While the Levant Basin in the southern sector has been extensively studied for hydrocarbon exploration, the northern domain offshore Cyprus, Turkey, Syria, and Lebanon remains less understood. In this study, we interpret a regional multichannel seismic reflection profile (MS56) in the time domain and then perform a time-to-depth conversion, supported by structural balancing, to build a crustal-scale geological model. Our reconstruction identifies three temporally constrained deformation stages—at the end of the Paleogene, an established accretionary wedge records the final phases of Tethyan subduction; during the Tortonian, strike-slip kinematics dominated, with sectors experiencing transtension or transpression and out-of-sequence thrusting in the outer wedge; and during the Messinian, continental collision was marked mainly by strike-slip deformation and regional uplift—revealing a progressive, diachronic evolution across the margin and the transition from subduction to continental collision. The Cenozoic evolution shows limited overall shortening, with deformation accommodated by out-of-sequence thrusting and strike-slip faulting. We reinterpret the Larnaka Ridge as a former extensional structure later inverted during Messinian transpression. At depth, the margin is structured by a basal detachment within Triassic evaporites, explaining the geometry of the accretionary wedge, topographic asymmetry, and structural vergence. The acoustic basement is interpreted as a composite of obducted ophiolitic slices and thinned continental crust. These findings provide a time-calibrated crustal model for the Cenozoic evolution of the northern Eastern Mediterranean.

Plain Language Summary The Eastern Mediterranean is a captivating region where the African, Arabian, and Eurasian tectonic plates have interacted for millions of years. While the southern part, such as the Levant Basin, has been extensively studied due to oil and gas exploration, the northern area remains less understood. This region is geologically active, with movements like stretching, squeezing, and sliding shaping its landscape. In this study, researchers utilized vintage seismic data to understand how the basins between Cyprus, Turkey, Syria, and Lebanon formed over the past 65 million years. They discovered that most of the major tectonic collisions occurred earlier, and the recent geological activity has largely involved sliding along old fault lines. This research enhances our understanding of how the Earth's surface in this region has changed over time.

Key Points:

- The Eastern Mediterranean's tectonic history involves interactions among the African, Arabian, and Eurasian plates since the Paleozoic era
- An analysis of seismic profile MS56 examined the Cenozoic basin's development in Cyprus, Turkey, Syria, and Lebanon
- The study found minimal Cenozoic shortening, as the main convergence phase had already ended

Supporting Information:

Supporting Information may be found in the online version of this article.

Correspondence to:

B. Lorenzo,
lbonini@units.it

Citation:

Nicolò, B., Lorenzo, B., Ben Anna, D., Giuseppe, B., Angelo, C., Edy, F., & Andrea, P. G. (2026). Cenozoic evolution of the North-Eastern Mediterranean Basins. *Tectonics*, *45*, e2025TC008896. https://doi.org/10.1029/2025TC008896

Received 27 FEB 2025
Accepted 14 DEC 2025

Author Contributions:

Conceptualization: Bertone Nicolò, Bonini Lorenzo, Camerlenghi Angelo
Data curation: Bertone Nicolò, Brancatelli Giuseppe, Forlin Edy
Formal analysis: Bertone Nicolò
Investigation: Bertone Nicolò, Camerlenghi Angelo
Methodology: Bertone Nicolò, Bonini Lorenzo, Brancatelli Giuseppe, Forlin Edy
Software: Bertone Nicolò
Supervision: Bonini Lorenzo
Validation: Bertone Nicolò, Bonini Lorenzo, Camerlenghi Angelo
Visualization: Bertone Nicolò
Writing – original draft: Bertone Nicolò, Bonini Lorenzo

1. Introduction

The Anatolia, Arabian, and African (Nubian) tectonic plates meet in the region of the Eastern Mediterranean Sea (Figure 1). Here, the convergence of the African and Anatolian plates created a complex tectonic system called the Cyprus Arc System (see e.g., Symeou et al., 2018) due to the subduction of the Neo-Tethys oceanic lithosphere under the Anatolian Plate during the Mesozoic and Cenozoic ages (e.g., Biju-Duval & Montadert, 1977; Kempler & Garfunkel, 1994; Vidal et al., 2000; Netzeband et al., 2006; Segev et al., 2018; Woodside, 1977).

The present-day Cyprus Arc System can be divided into three different sectors, from west to east: (a) the Florence Rise, (b) the Cyprus Arc, and (c) the Latakia Ridge (Figure 1). The kinematics and geometry of the structures in these three sectors differ because of the nature of the different crustal domains. At the southern edge of the Florence Rise, the subducting plate is a continuation of the Herodotus Basin and is composed of oceanic crust (Figure 1; Granot, 2016). Moving eastward, south of the Cyprus Arc and the Latakia Ridge, the subducting plate is composed mainly of thinned continental crust (Levant basin; Figure 1; Granot, 2016; Steinberg et al., 2018)

Writing – review & editing: Bertone Nicolò, Bonini Lorenzo, Brancatelli Giuseppe, Camerlenghi Angelo, Forlin Edy

hosting isolated thicker blocks (e.g., Eratosthenes Seamount; Figure 1; Mart & Robertson, 1998; Robertson, 1998b; Welford et al., 2015).

Consistent differences also characterize the overriding plate north of the Cyprus Arc System. North of the Florence Rise, the Antalya Basin represents a wide forearc basin (Figure 1; e.g., Noda, 2016). In the sector of Cyprus Arc, Cyprus Island is a result of the complex contractional assembly of allochthonous units, including the Troodos ophiolites (Figure 1; e.g., Moix et al., 2007; Robertson et al., 2012). The offshore area between Cyprus Island and Syria/Lebanon (Figure 1), north of the Latakia Ridge, features two prominent ridges, Larnaka and Margat, along with neighboring basins known as Cyprus and Latakia basins. Moving northward, another important submarine ridge known as the Kyrenia Ridge and its continuation on land as the Kyrenia Range on Cyprus Island delineate the southern boundary of the Cilicia Basin (Figure 1).

It is worth noting that the easternmost sector of the Cyprus Arc System has been influenced by the left-lateral transcurrent activity of the Dead Sea Transform Fault, which, since the Miocene, has partitioned the convergence between the Arabian and African plates. This influence is expressed by the development of strike-slip structures and oblique deformation patterns in the Latakia Ridge and surrounding areas (Hempton, 1987; Vidal et al., 2000).

Several works have described and discussed the geometry and tectonic evolution of the main tectonic structures in this eastern sector, utilizing various methods such as seismic reflection profiles (Alsouki et al., 2019; Ben-Avraham et al., 1995; Kempler & Garfunkel, 1994; Symeou et al., 2018; Vidal et al., 2000), seismic refraction data (Feld et al., 2017), gravimetric models (Ergün et al., 2005; Khair & Tsokas, 1999; Sampietro et al., 2018), numerical models (Fernàndez-Blanco et al., 2020), and other techniques like field data (Papadimitriou et al., 2018).

This study aims to improve the understanding of the crustal architecture and the structural evolution of this geodynamically complex region by providing a detailed description of the geometry, kinematics, and timing of primary structures by thoroughly reevaluating the information yielded by an existing, vintage seismic reflection profile.

Between 1969 and 1982, as part of an Italian scientific program focused on exploring the entire Mediterranean Sea, the National Institute of Oceanography and Applied Geophysics (OGS), at the time named Osservatorio Geofisico Sperimentale (OGS), conducted a series of multichannel seismic reflection surveys aboard the National Council of Research's ship “Marsili” (MS Project—Finetti & Morelli, 1973). The deep-penetration seismic profile MS56, approximately 571 km long, crosses the Eastern Mediterranean Sea from the southern Turkish coast to the Nile Delta (Figure 1), with a penetration of about 10 s two-way travel time (TWT).

In this study, the original MS56 profile was reprocessed using updated seismic workflows (Brancatelli et al., 2022) to enhance resolution and eliminate multiple reflections, thereby enabling more detailed structural and stratigraphic analysis. Our focus is on identifying key seismic-stratigraphic packages and tectonic features. Using the seismic velocity from processing, we create a pre-stack depth-migrated geological section of the shallower crustal levels. This section serves as a constraint for a crustal model that incorporates published data on basement and Moho depth. Compared to other seismic data sets in the region—particularly those in the deformed basins north of the Cyprus Arc (e.g., Aksu et al., 2021; Calon et al., 2005; Hall, Aksu, et al., 2005; Hall, Calon, et al., 2005)—which mainly offer shallower coverage and consist of shorter, denser lines, MS56 provides a unique blend of deep penetration and broad regional coverage. This enables the imaging of geological features, such as the top Cretaceous unconformity and deeper crustal structures, that are not accessible with other available 2D seismic lines. As a result, it facilitates correlation across multiple basins on a regional scale.

2. Geological Setting

The current geodynamic setting of the Eastern Mediterranean results from the complex interactions among the African, Anatolian, and Arabian plates (Figure 1). Tectonic evolution has been heavily shaped by the subduction of the Neo-Tethys oceanic lithosphere beneath the Anatolian Plate, leading to the development of the Cyprus Arc System (e.g., Biju-Duval & Montadert, 1977; Kempler & Garfunkel, 1994; Netzeband et al., 2006; Segev et al., 2018; Vidal et al., 2000; Woodside, 1977). This system is divided into three main segments—Florence Rise, Cyprus Arc, and Latakia Ridge—each with unique crustal characteristics and tectonic styles (Granot, 2016; Steinberg et al., 2018; Mart & Robertson, 1998; Welford et al., 2015—Figure 1). The western segment is

10.1029/2025TC008896

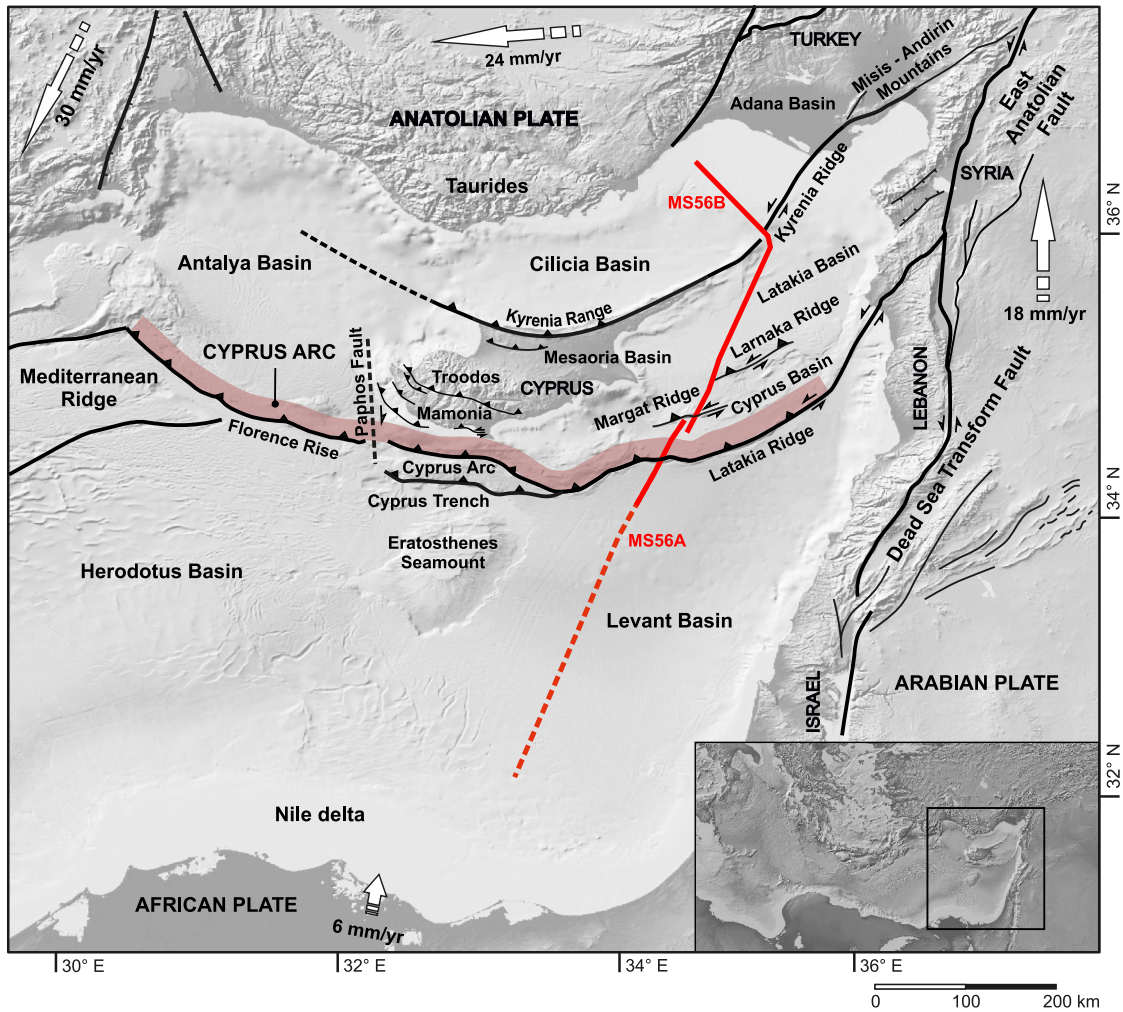

Figure 1. Tectonic map of the Eastern Mediterranean Sea. Red lines represent the interpreted portion of the MS56 seismic section; the red dashed line represents the remaining portion of the MS56 seismic section not considered in this study. White arrows are the GPS velocity of the plates from McClusky et al. (2000). Tectonic lineaments from Montadert et al. (2014), Longacre et al. (2007), and McPhee and van Hinsbergen (2019). Maps are from GeoMapApp (n.d.) (http://www.geomapapp.org).

dominated by the subduction of oceanic crust from the Herodotus Basin, while the central and eastern segments mainly involve thinned continental crust, with isolated thicker blocks such as the Eratosthenes Seamount (Granot, 2016; Mart & Robertson, 1998; Robertson, 1998b; Steinberg et al., 2018). Structurally, the region displays a superposition of extensional, contractional, and strike-slip tectonic phases (Kempler & Garfunkel, 1994). The extensional phase, linked to continental crust thinning and the opening of Neo-Tethys, occurred from the Early Triassic to the Late Jurassic (Ben-Avraham et al., 1995; Frizon de Lamotte et al., 2011; Gardosh et al., 2010; Garfunkel, 2004). It was followed by a contractional phase, starting in the Cretaceous, which was responsible for forming the Cyprus Arc System through subduction-related processes. Since the Miocene, the opening of the Red Sea and the propagation of the Dead Sea Transform Fault, driven by the northward movement of the Arabian Plate relative to the African Plate, have triggered westward escape tectonics of the Anatolian Plate and regional tectonic reorganization (Faccenna et al., 2006; Hempton, 1987; Moix et al., 2007; Morris et al., 2006; Schattner & Ben-Avraham, 2007; Van Hinsbergen et al., 2020). Currently, while subduction remains active beneath the Florence Rise and Cyprus Arc (Güvercin et al., 2021; Robertson, 1998a), the Latakia and Kyrenia Ridges show a transition from pure convergence to transpressional regimes, characterized by strike-slip reactivation of inherited faults (Figure 1—Vidal et al., 2000; Hall, Aksu, et al., 2005; Hall, Calon, et al., 2005; Symeou et al., 2018).

2.1. Stratigraphic Setting

Knowledge of the stratigraphy in different parts of the study area varies based on the availability of data. In particular, the presence of offshore exploration wells is crucial to correctly interpreting the seismic facies along a seismic profile. In the following sections, we will summarize the stratigraphy of the basins that our seismic profile passes through. To incorporate the limited stratigraphic data from exploration wells in the offshore area, we will also outline the stratigraphy of the nearest onshore sector, which is Cyprus Island.

2.1.1. Cyprus

Cyprus Island comprises three sectors, from north to south: the Kyrenia Range, the Troodos Complex, and the Mamonia Terrain (Figure 1).

The Kyrenia Range is a southward-verging allochthonous mountain range seen as a part of the outermost Taurides (Robertson & Kinnaird, 2016). This zone comprises a series of deformed and recrystallized limestones and dolomites of the Permian to Early Cretaceous age, followed by sedimentary rocks from the Late Cretaceous to Miocene age, along with Upper Cretaceous volcanic intrusion (Chen & Robertson, 2021; Robertson & Kinnaird, 2016).

The Troodos Complex is a one-of-a-kind ophiolite sequence, regarded as one of the most comprehensive ophiolite series in the world (Moores & Vine, 1971). It is a fragment of oceanic crust formed about 90 Ma in an oceanic setting above a subduction zone, consistent with a supra-subduction origin for the Troodos ophiolite (Dilek & Robinson, 2003; Miyashiro, 1974; Moix et al., 2007; Pearce, 2003; Pearce & Robinson, 2010; Taylor et al., 2022). Subsequently, this newly formed oceanic crust was obducted, uplifted, and eroded starting from the Maastrichtian (e.g., Robertson et al., 2012). These processes led to a dome-shaped complex with a lower suite of rocks in its core and stratigraphically younger rocks on the flanks (Maffione et al., 2017; Ring & Pantazides, 2019).

The Mamonia Terrain is an allochthonous fragment of continental crust made of igneous, sedimentary, and metamorphic rocks ranging from the Triassic to Late Cretaceous age (Malpas et al., 1992; Moix et al., 2007; Robertson & Woodcock, 1979). It represents an assemblage of allochthonous units accreted during subduction processes. These rocks appear strongly deformed and are mixed with large portions of the Troodos ophiolites, forming a vast mélange zone interpreted as an accretionary complex composed of disrupted and imbricated sedimentary and oceanic lithologies, which formed in response to subduction-related processes and provides crucial evidence for the tectonic assembly of Cyprus (Bragin et al., 2021; Festa et al., 2010; Lapierre et al., 2007).

The Cenozoic sedimentary cover in all three sectors includes shales, volcaniclastites, marls, chalks, cherts, limestones, calcarenites, and evaporites (Harrison et al., 2004; Kinnaird & Robertson, 2013).

2.1.2. Levant Basin

The nature of the basement underlying this basin is uncertain. Based on seismic refraction data, some authors have inferred that the basement consists of thinned continental crust (Granot, 2016; Longacre et al., 2007; Smaily, 2017) underneath approximately 12 km of sediments (Montadert et al., 2014). Information on the sedimentary cover derives from boreholes, seismic reflection profiles and outcrops along the southeastern edge (Figure 2; see, e.g., Gao et al., 2019; Gardosh & Druckman, 2006; Gardosh et al., 2008; Ghalayini et al., 2018; Hawie et al., 2013; Nader et al., 2018; Robertson, 1998b; Segev et al., 2018). The oldest drilled rocks are Upper Triassic to Lower Jurassic shallow marine carbonates and siliciclastics reached offshore in Israel (Figure 2) (Gardosh et al., 2008). Lower and Upper Triassic evaporites and carbonate rocks have been suggested for the deeper section of the sedimentary cover (Ghalayini et al., 2018). Middle Jurassic rocks consist of thick platform carbonates (Gardosh et al., 2008; Ghalayini et al., 2018). Late Jurassic deposits is made of platform and pelagic carbonates overlain by an Early Cretaceous sequence of pelagic carbonates with layers of shales and sands in between (Gardosh et al., 2008; Ghalayini et al., 2018). The Upper Cretaceous-Paleocene rocks comprise pelagic chalk, shales, and turbidites (Gardosh et al., 2008; Ghalayini et al., 2018), overlain by Eocene marly limestones with conglomerates in the upper part (Gardosh et al., 2008; Ghalayini et al., 2018). From the Oligocene to the Miocene, mudstone deposition is interbedded by sandy/calcareous turbidites (Gardosh et al., 2008). During the Late Miocene (Messinian), a thick layer of evaporites was deposited in the basin. At the same time, the margin was affected by erosion, and the sediments were transported into the basin along deeply incised canyons (Druckman et al., 1995), resulting in an alternation of pure halite, anhydrite, and shale layers (Feng et al., 2016;

10.1029/2025TC008896

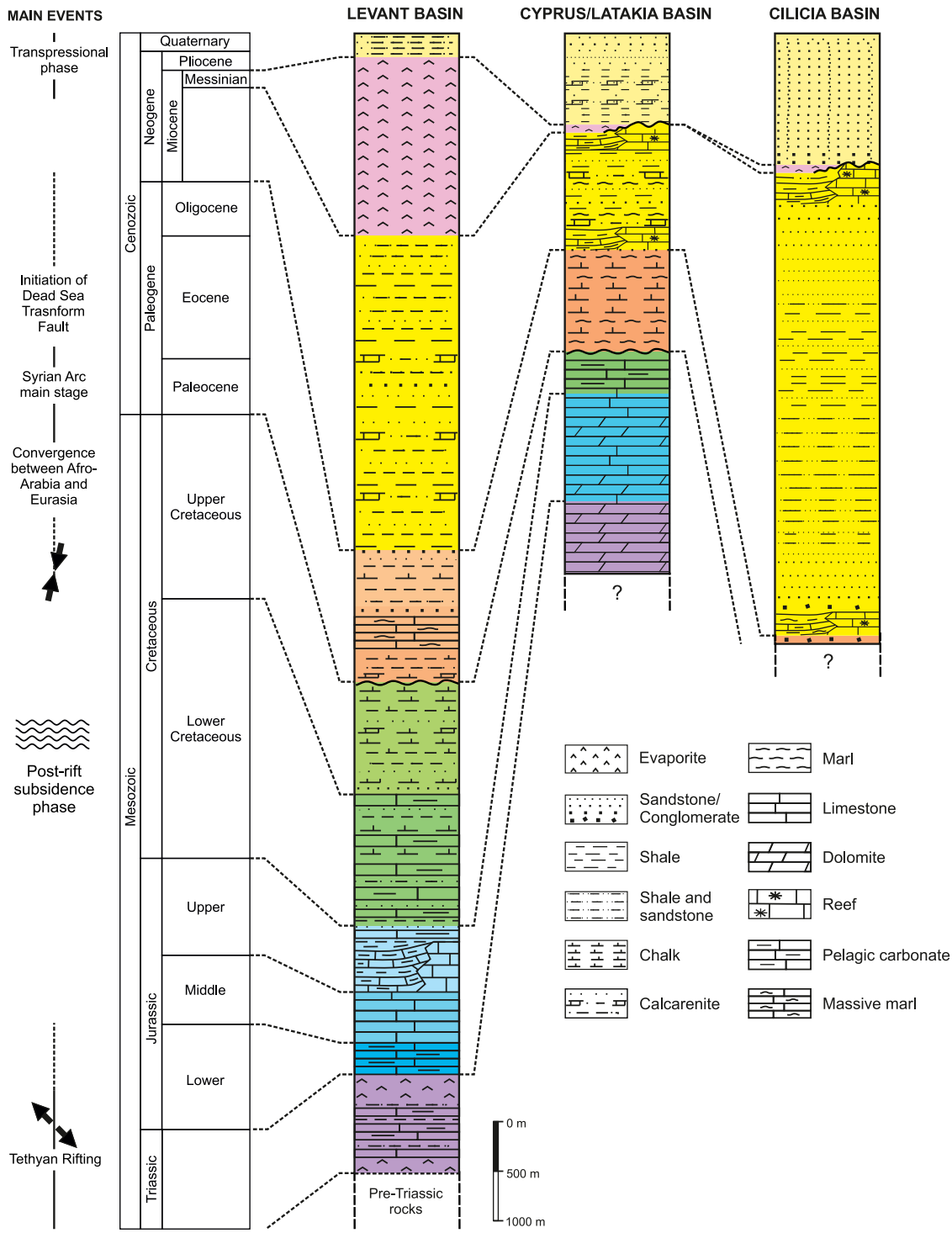

Figure 2. Simplified stratigraphic column of the study area. For the Levant Basin, data from Hawie et al. (2013), Ghalayini et al. (2018), Nader et al. (2018), and Gao et al. (2019). For the Cyprus and Latakia basins, data from McCay and Robertson (2013), Papadimitriou et al. (2018), Follows (1992); Bilim et al. (2017), and Bowman (2011). For Cilicia—Adana basins, data from Çíftçí et al. (2012).

Gvirtzman et al., 2017). The Plio-Quaternary succession is made of hemipelagic clay and marl (e.g., Hawie et al., 2013; Montadert et al., 2014).

2.1.3. Cyprus and Latakia Basins

The stratigraphy of these basins is derived from published Syrian coastal boreholes (Figure 2; Bowman, 2011; Bilim et al., 2017) and the outcropping rocks and borehole data in the Mesaoria Basin (McCay & Robertson, 2013). No publicly available boreholes exist for these basins.

The nature of the basement of the Cyprus–Latakia basins is still a matter of debate, as no direct data are available. Some boreholes from the Syrian margin drill Cretaceous carbonates, and the Ayse-1 well in the Iskenderun Basin targets the Neotethyan ophiolites, which are directly overlain by Miocene sediments (Bowman, 2011). Rybakov et al. (2011) created the most detailed map of magnetic anomalies in the study area. They analyzed the magnetic anomalies in the northeastern Mediterranean Sea, distinguishing between those related to volcanic intrusion and those associated with obducted ophiolites, thus ruling out the presence of a single massive ophiolite beneath the "deformed basins." The Iskenderun Basin drills the Neotethyan ophiolites, which are directly overlain by Miocene sediments (Bowman, 2011). Rybakov et al. (2011) realized the most detailed map of magnetic anomalies in the study area. They analyzed the magnetic anomalies in the northeastern Mediterranean Sea, separating the anomalies related to volcanic intrusion from those related to the obducted ophiolites, ruling out the presence of a unique massive ophiolite beneath the "deformed basins."

The older rocks described are Triassic-Jurassic dolomites and limestones (Bowman, 2011). The carbonate succession ends in the Cretaceous with pelagic carbonates (Bowman, 2011). The Paleocene rocks consist of pelagic chalks and marls, becoming partially massive in the Oligocene-Eocene (Papadimitriou et al., 2018). The Lower Miocene is characterized by reef and pelagic carbonates, which are covered by the Middle Miocene's marls, shales, calcarenites, and conglomerates (Follows, 1992). The Tortonian rocks comprise reef and pelagic carbonates, passing upwards into Messinian evaporites (Follows, 1992). The sharp sea-level fall of the Messinian Salinity Crisis led to the deposition of evaporites in the basins and the erosion on the margins and paleogeographic highs (Maillard et al., 2011). The Plio-Quaternary sequence consists of hemipelagic shale, calcarenites, and coarser siliciclastic sediments (e.g., Calon et al., 2005; Symeou et al., 2018).

2.1.4. Cilicia Basin

Data on the Cilicia Basin stratigraphy (Figure 2) derive from exploration wells and onshore outcropping rocks in the adjacent Adana Basin (Çíftçí et al., 2012).

The known stratigraphic sequence starts with Oligocene continental conglomerates and sandstones, followed by a Miocene thin layer of reef limestones and pelagic marls that pass upward into shales and sandstones (Çíftçí et al., 2012). The Upper Miocene rocks consist of reef limestones and pelagic marls and shales (Çíftçí et al., 2012). The deposits related to the Messinian Salinity Crisis are thinner in the Adana Basin than in the southern basins and consist of gypsum with minor sandstones and shales, passing to halite with anhydrite intercalations (Çíftçí et al., 2012).

The succession ends with Plio-Quaternary conglomerates and sandstones that pass upwards into the poorly consolidated Quaternary clastics (Çíftçí et al., 2012).

3. Data and Method

The primary data used for this study is the seismic reflection profile MS56 belonging to the MS data set (Mediterranean Sea project—Finetti & Morelli, 1973). This seismic line was acquired in 1973 using a dynamite FLEXOTIR marine seismic source and a 24-channel, 2,400 m-long analog seismic streamer. It was planned for deep penetration with a record length of 10 s (Table 1; Figure 3).

3.1. Seismic Data and Processing

In recent years, a significant portion of the MS data set has been carefully reprocessed, renewing its scientific value (Brancatelli et al., 2022; Camerlenghi et al., 2019; Civile et al., 2021). A state-of-the-art broadband processing workflow was applied to the MS56 profile to improve the signal-to-noise ratio by reducing both coherent

Table 1
Acquisition Parameters of the MS56 Seismic Sections

Seismic lines	MS56-A/B
Recording date	1973
Lines total length	571 km
Streamer length	2,400 m
Number of channels	24
Near offset	270 m
Group interval	100 m
Recording filters	10–72 Hz
Seismic source	Dynamite—FLEXOTIR
Fold	1,200%
Record length	10 s
Sampling interval	4 ms

and incoherent noise. The results show a marked improvement in resolution and signal clarity compared to the original vintage data. A similar processing sequence, with detailed explanations of each step, is described in the works of Brancatelli et al. (2022), Camerlenghi et al. (2019), and Civile et al. (2021). The main processing steps included:

1. *Deghosting* to recover lost frequencies and extend the bandwidth, enhancing temporal resolution.
2. *Attenuation of surface-related multiples* using standard techniques, such as Surface Related Multiples Elimination (SRME; Verschuur et al., 1992), can be improved by interpolating shots and receivers to achieve better spatial coverage.
3. *Integration of SRME with Wave Equation Multiple Attenuation* (*WEMA*; *Wiggins*, 1988) to further suppress residual multiples. In particularly noisy zones, this was supplemented with Water Bottom Predictive Deconvolution or Radon filtering.
4. *Predictive surface-consistent deconvolution*, applied to account for variations in the source signature. This improvement enhanced data quality by reducing noise, stabilizing amplitudes, and improving vertical resolution and reflector continuity.
5. *Pre-stack Kirchhoff time migration*, performed iteratively with continuous velocity updates. Each iteration included quality control based on common-distance stack analysis.
6. *FX deconvolution*, followed by time-variant filtering and trace amplitude equalization, aimed at improving lateral reflector continuity on the pre-stack time-migrated (PSTM) section while reducing noise and enhancing signal strength.

Overall, this reprocessing significantly improved seismic data quality, enabling:

- Better characterization of seismic facies;
- More reliable imaging of subsurface structures;
- Improved detection and interpretation of fluid-related amplitude anomalies;
- Higher resolution across the data set.

Despite limitations such as low fold coverage and noisy gathers, the vintage data were processed to their fullest potential, resulting in a substantial enhancement in quality and interpretability.

3.2. Seismic Interpretation

The first phase of the seismic interpretation, performed on the time-migrated section, is devoted to identifying the main seismic facies and assigning them a stratigraphic meaning, taking insights from previous studies on the Cypriot, Turkish, Lebanese, and Syrian areas (Bowman, 2011; Calon et al., 2005; Ghalayini et al., 2014; Hawie et al., 2013; Çíftçí et al., 2012). During this phase, we emphasize the reflectors that separate sequences useful to reconstruct the tectonic evolution of the study area from the Upper Cretaceous to the present day.

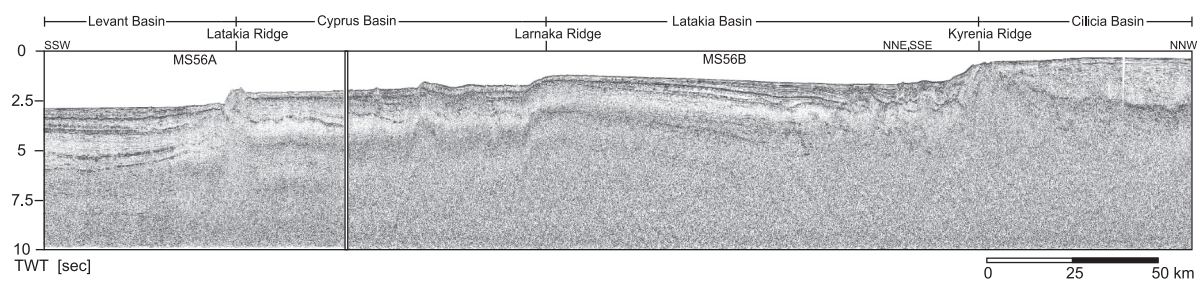

Figure 3. Part of the MS56A and MS56B seismic sections. The MS56B has been reprocessed, and both are time-migrated, positioned in Figure 1.

Table 2
Velocity and Gradient Values Used for the Depth Conversion of the MS56 Seismic Section

Seismic package	Velocity [m/s]	Velocity gradient [Hz]
Water	1,520	0
Plio-Quaternary	2,000	0.1
Messinian	4,100	0
Miocene + Paleogene	3,150	0.1
Acoustic basement	3,500	0.2

3.3. Crustal Modeling

When the seismo-stratigraphic units and the principal tectonic structures are identified, we convert our interpreted reflectors and units of the time-migrated section from two-way travel time (TWT) to depth domains using the following equation:

$$Z_x = v_0 \frac{e^{kt} - 1}{k}$$

where Z is the thickness of a layer x, corresponding to an individual seismic package with an initial interval velocity v_0 (m/s), k (H_z) is the rate of velocity change with depth, and t is the one-way travel time (second).

To derive interval velocities for the depth conversion, we used the results of velocity analyses performed on the MS56 seismic data set, supported by published data (Calon et al., 2005; Klaeschen et al., 2005). For each interpreted seismic unit, we calculated the average interval velocity and its vertical gradient, which were then assigned to corresponding polygons in MOVE software (Table 2). These velocity models were subsequently applied to both the SEG-Y data and the interpreted line drawings in two-way travel time (TWT), yielding a depth-converted seismic section and stratigraphic horizons.

The crustal model is finally used to reconstruct the main evolutionary stages of the area from the end of the Paleogene.

4. Results and Seismic Interpretations

This chapter presents the main results of the seismic interpretation and the derived geometrical framework. The analysis combines descriptive observations of seismic facies with basic interpretative elements required to define the key horizons and to perform the time-to-depth conversion. Broader tectonic implications are discussed in Chapter 5.

4.1. Interpretation of Seismic Facies and Key Horizons

As the first step in seismic interpretation, we identified five main horizons that separate different seismic packages (Figure 4). Starting from the top, the first package exhibits high amplitude and frequencies, characterized by sub-horizontal, continuous, and parallel reflectors, which are well visible throughout the entire section. We interpreted it as the Plio-Quaternary terrigenous sequence. It is typically based on a strong positive reflector (H1 in Figure 4), which is given by the high acoustic impedance contrast between the overlying terrigenous sediments and the underlying evaporites, or, especially in the upper slopes, it represents an evident erosional truncation.

Below H1, a second seismic package is identified on a high-amplitude reflector with reverse polarity (H2) with respect to the seafloor reflector. Its uppermost seismic unit is chaotic with high amplitude and frequencies. Its central unit also presents chaotic seismic facies interspersed with strongly deformed reflective layers. Its lower unit has continuous and parallel reflectors. The entire sequence is interpreted as Messinian evaporites, a high-velocity medium generally identified by peculiar strong reflectors, with positive polarity at their top and negative polarity at its base (e.g., Camerlenghi et al., 2019; Feng et al., 2016).

Below the Messinian sequence, continuous parallel reflectors characterize the third seismic sequence, where different seismic facies are evident along the seismic section. In the Levant Basin, the upper and lower units are represented by undulating low- to high-amplitude reflectors separated by a high-amplitude seismic package composed of a triplet of parallel reflectors. A strong reflector is present at the base of the sequence (Figure 4). The triplet represents a key marker, well visible throughout the Levant Basin. In the Cyprus and Latakia basins, the basal reflector H3 is characterized by high amplitude and low frequencies and passes into less reflective facies in the central part. In the Cilicia Basin, this sequence comprises several chaotic and lenticular bodies that flow down from the Kyrenia Ridge and downlap onto the deeper sequence. It is related to the Miocene, which is composed of deep marine sediments.

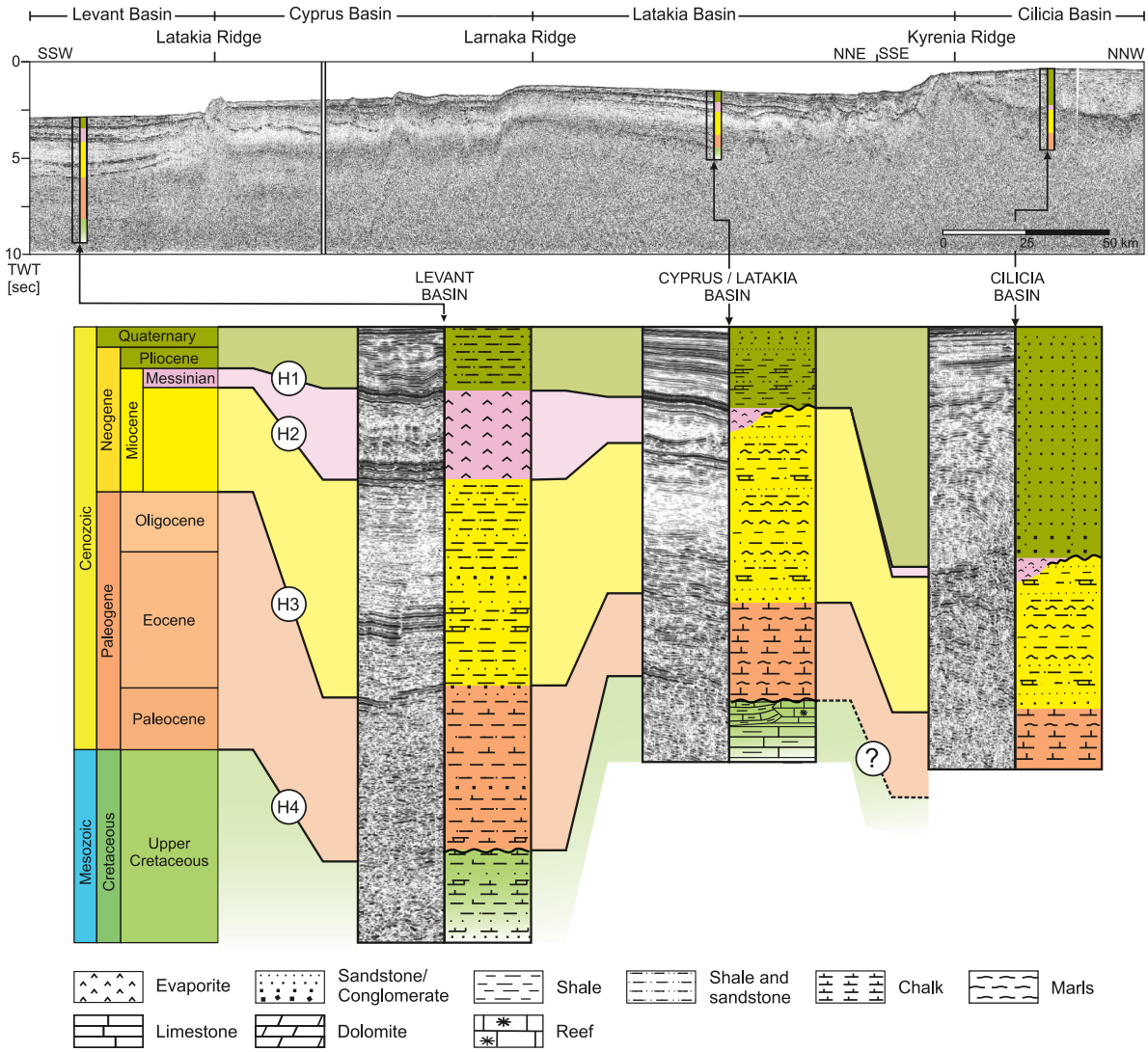

Figure 4. Seismic facies of the interpreted horizons and relative seismic packages of the MS56 seismic section. The main horizons are H1—base of the Plio-Quaternary seismic package, H2—base of the Messinian seismic package, H3—base of the Miocene seismic package and H4—base of the Paleogene seismic package.

Below H3, the seismic facies in the Levant and Cilicia basins are chaotic and not well-resolved (Figure 5). Locally, some coherent high-amplitude and low-frequency signals are visible. In the Cyprus and Latakia basins, the resolution is higher, with low to medium amplitude south of the Larnaka Ridge and higher amplitude to the north (Figure 4). The whole sequence, related to the Paleogene sequence, mainly composed of chalks and marls, represents a wedge that onlaps the continuous high amplitude and low-frequency basal reflectors H4. This last represents the boundary between the Paleogene sequence and the Upper Cretaceous deposits.

The signal-to-noise ratio decreases below H4. In the MS56 seismic section, some scattered deep reflections are interpreted as being at the top of the carbonate platform (Figures 6a and 6b).

4.2. Interpretation of the Sedimentary and Tectonic Structures

As mentioned, our seismic profile crosses different basins of the Eastern Mediterranean. In the following sections, the interpretation of each basin is subsequently merged for a general overview of the sedimentary and tectonic structures along the regional seismic profile.

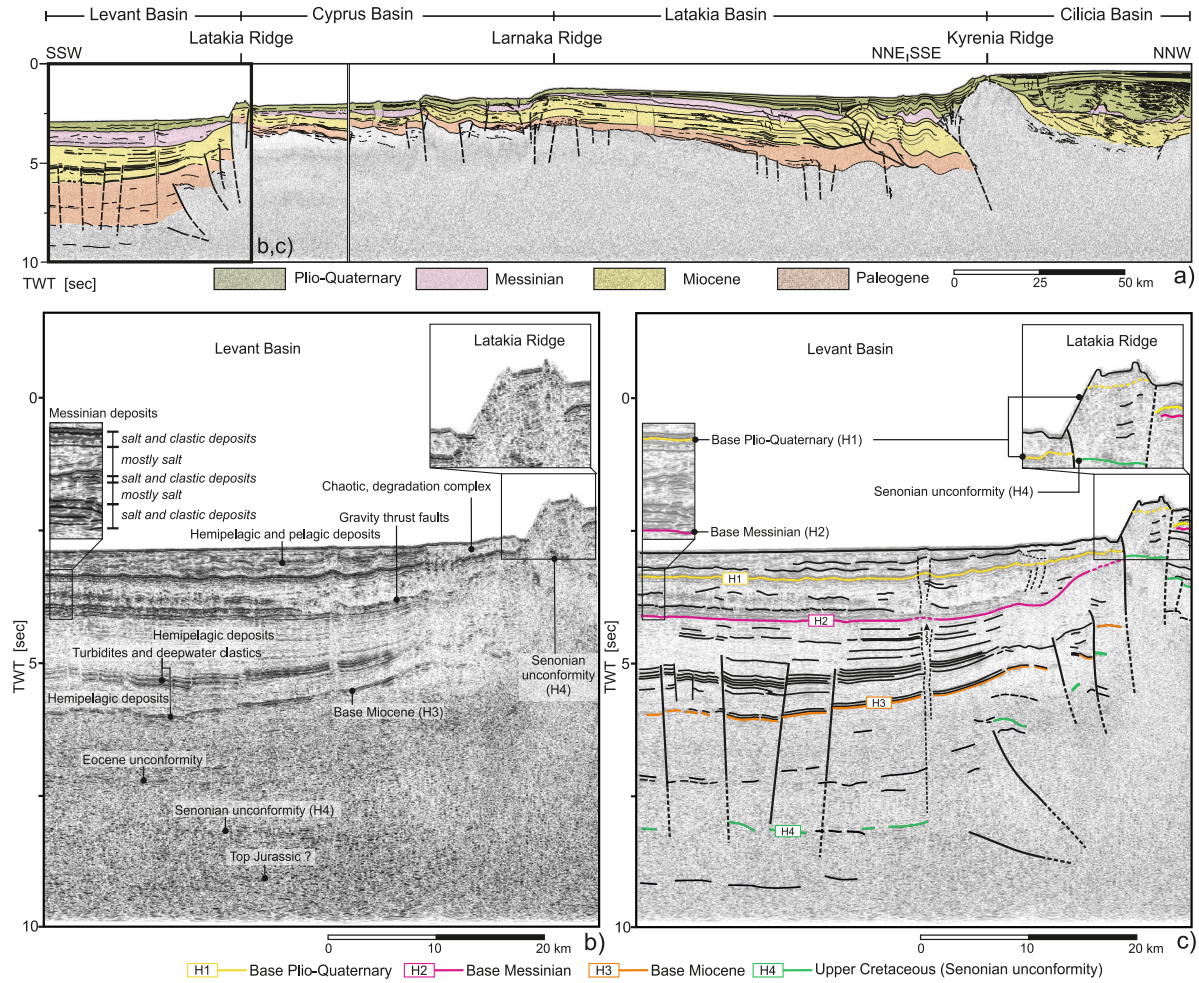

Figure 5. (a) Interpretation and line-drawing overlay on the MS56 TWT seismic section. (b) Zoom of the southern part of the seismic section, imaging the northern Levant Basin and the Latakia Ridge without the line drawing, and (c) interpreted.

4.2.1. Levant Basin

In our seismic profile (Figure 5), the Plio-Quaternary deposits in the Levant Basin area have a slightly constant thickness in the southern zone and become thinner approaching the Latakia Ridge. The seismic sequence can be interpreted as hemipelagic and pelagic deposits in the south-central zone. Conversely, south of the Latakia Ridge, the chaotic seismic facies are probably linked to erosion of the uplifting Ridge and re-sedimentation in front of its slope. The Plio-Quaternary deposits seem thinner above the Latakia Ridge (see inset in Figure 5c). A high-angle fault borders the Ridge.

Below the Plio-Quaternary deposits, there is a thick sequence of Messinian evaporites. In the Levant Basin area, the evaporites have internal reflections due to an alternation between salt (transparent facies) and salt mixed with clastic deposits (reflective layers; Figure 5). This alternation influences its rheological behavior resulting in internal multiple detachment levels, with gravity-induced structures, such as extensional faults close to the Latakia Ridge and thrusts moving toward the basin (Figure 5). On the Latakia Ridge the Messinian deposits are not present.

The seismic data shows that the Miocene deposits appear as parallel and continuous reflectors, which we interpret as hemipelagic deposits. In the middle of this package, the high-amplitude triplet of turbidite deposit and the high-amplitude Miocene base allow the interpretation of different high-angle extensional faults. As for the Plio-Quaternary and Messinian deposits, the Miocene succession becomes thinner as it approaches the Latakia Ridge. Reverse faults control this thickness variation, which is detected south of the Latakia Ridge.

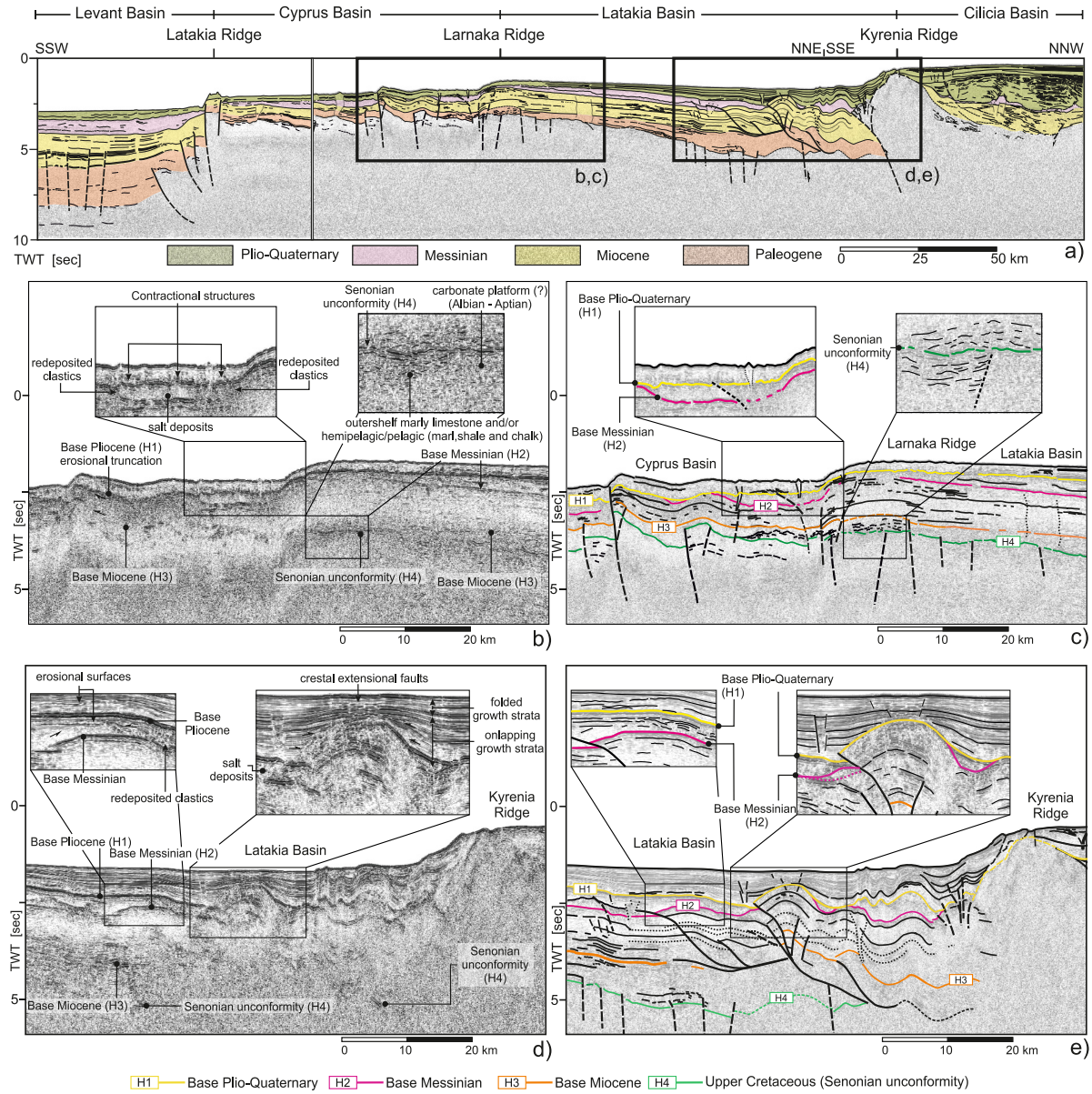

Figure 6. (a) Interpretation and line-drawing overlay on the MS56 TWT seismic section. (b) Zoom of the central part of the uninterpreted seismic section imaging the Larnaka Ridge area. (c) Interpreted zoom of the central part of the MS56 seismic section imaging the Larnaka Ridge area. (d) Zoom of the northern part of the MS56 uninterpreted seismic section imaging the southern portion of the Kyrenia Ridge and the northern Latakia Basin area. (e) Interpreted zoom of the southern portion of the Kyrenia Ridge and the northern Latakia Basin area.

Due to its depth and residual multiple reflections, the Paleogene package characterizes a degraded seismic signal. However, some reflectors can be highlighted. In particular, we recognize the Senonian unconformity (H4) displaced by thrust faults, which produces large variability in the Paleogene thickness and the throw of the H4 reflector, corresponding to 2–3 s (TWT) at the Latakia Ridge with respect to the southern region.

4.2.2. Cyprus and Latakia Basins

In the Cyprus Basin, the Plio-Quaternary sequence has a quite constant thickness. Conversely, in the Latakia Basin, especially close to the Kyrenia Ridge, it thickens northward (Figure 6). At the top of the Larnaka Ridge, the thinning of the Plio-Quaternary deposits is due to the gliding of the Messinian evaporites (Figures 6a–6c). South of the Kyrenia Ridge, the Plio-Quaternary deposits show growth strata and crestal extensional faults coinciding

with prominent contractional folds (Figures 6a, 6d, and 6e). On the top of the ridge, the Plio-Quaternary thickness is smaller and folded, testifying the recent tectonic uplift.

Below the Plio-Quaternary sequence, the Messinian deposits are discontinuous, marked by transparent facies of salt deposits in the center of the two depressions and by chaotic facies at their borders, due to redeposited sediments derived from the erosion of the structural highs. In the Larnaka Ridge, the Messinian package appears thinned at the top of the structure due to the gliding of the salt toward the south, where an isolated Messinian minibasin shows internal contractional systems due to sediment/evaporite load (see insets in Figures 6b and 6c). South of the Kyrenia Ridge, in the most prominent contractional fold (upper right inset in Figures 6d and 6e), the Messinian deposits are absent. The Miocene deposits are thinner in the Cyprus Basin than in the Latakia Basin, with an abrupt change across the Larnaka Ridge (Figure 6); hence, on this ridge, Miocene deposits have a reverse thickness relationship with respect to the Messinian and the Plio-Quaternary ones. This can be related to the change of kinematics (positive tectonic inversion) of Larnaka Ridge over time. During the Miocene, this ridge coincided with an extensional fault system that created a larger accommodation space in the northern sector. The thinning of Plio-Quaternary deposits and the gliding of Messinian evaporites mark an inversion of a Miocene basin since the Messinian and the Plio-Quaternary tectonic phases (Figures 6a and 6b). The Miocene thickness is approximately constant in the Latakia Basin, and the reflectors are quite parallel and continuous.

The Paleogene sedimentary wedge thickens from south to north and onlaps the Senonian unconformity H4.

In the Cyprus and Latakia basins, the H4 reflector is shallower than in the other basins, allowing the interpretation of some reflectors below it. For instance, some isolated carbonate build-ups and aggradations have been interpreted near the H4 highs (upper right inset in Figures 6b and 6c). The interpretation of the H4 reflector also allows the detection of the deeper roots of the faults and the extensional faulting active during the deposition of the Paleogene package.

4.2.3. Cilicia Basin

Along the interpreted seismic section, the Plio-Quaternary deposits reach the maximum thickness in the Cilicia Basin. H1 (base of the Plio-Quaternary sequence) and H2 (base of the Messinian sequence) are the only identifiable key reflectors in this basin. Below the Messinian seismic package, horizons are masked mainly by several multiple reflections of the shallow sea bottom. Therefore, the location of the H3 and H4 unconformities can only be hypothesized (Figure 7). The arrangement of the Plio-Quaternary horizons, showing differently tilted reflectors, together with the dislocation of the H1 and H2 unconformities, allows the recognition of still active extensional phase. The geometry of the Plio-Quaternary sediments depicts two roll-over anticlines (Figure 6c) with their antithetic master faults cutting the Messinian base. These faults are produced by the Messinian salt gliding from the borders of the basin toward the halokinetic structure in the middle, where salt accumulates.

At the northern flank of the Kyrenia Ridge, the Miocene deposits are onlapping, inclined, and partially eroded, testifying to an uplift of the ridge before the Messinian and continuing after.

4.3. Time-to-Depth Conversion and Crustal Model Building

The interpretation of the time-migrated section allowed us to better recognize the main tectono-stratigraphic features of the study area, while different key sectors provided insights into the kinematic evolution of the main structures.

As a first step in obtaining a crustal model, we converted our interpretation from travel time domain (TWT) to depth domain (Figure 8b). We assigned to each seismic package an interval velocity with a vertical gradient (Hz) to consider the natural velocity increasing with depth (Table 1 and Figure 8a). We then assigned 2,000 m/s and 0.10 Hz to the Plio-Quaternary package, 4,100 m/s and 0 Hz to the Messinian package, 3,150 m/s and 0.10 Hz to the Miocene/Paleogene package, and 3,500 m/s and 0.2 Hz to the deeper rocks (Figure 8b).

As a further step, we merged the two segments of the MS56 profile, obtaining a continuous seismic section by removing the overlapping sectors (Figure 8c). To focus on the tectonically active domain, we have not considered the undeformed central part of the Levant Basin, but only its northern portion near the Latakia Ridge, where compressional and transpressional deformation is most evident.

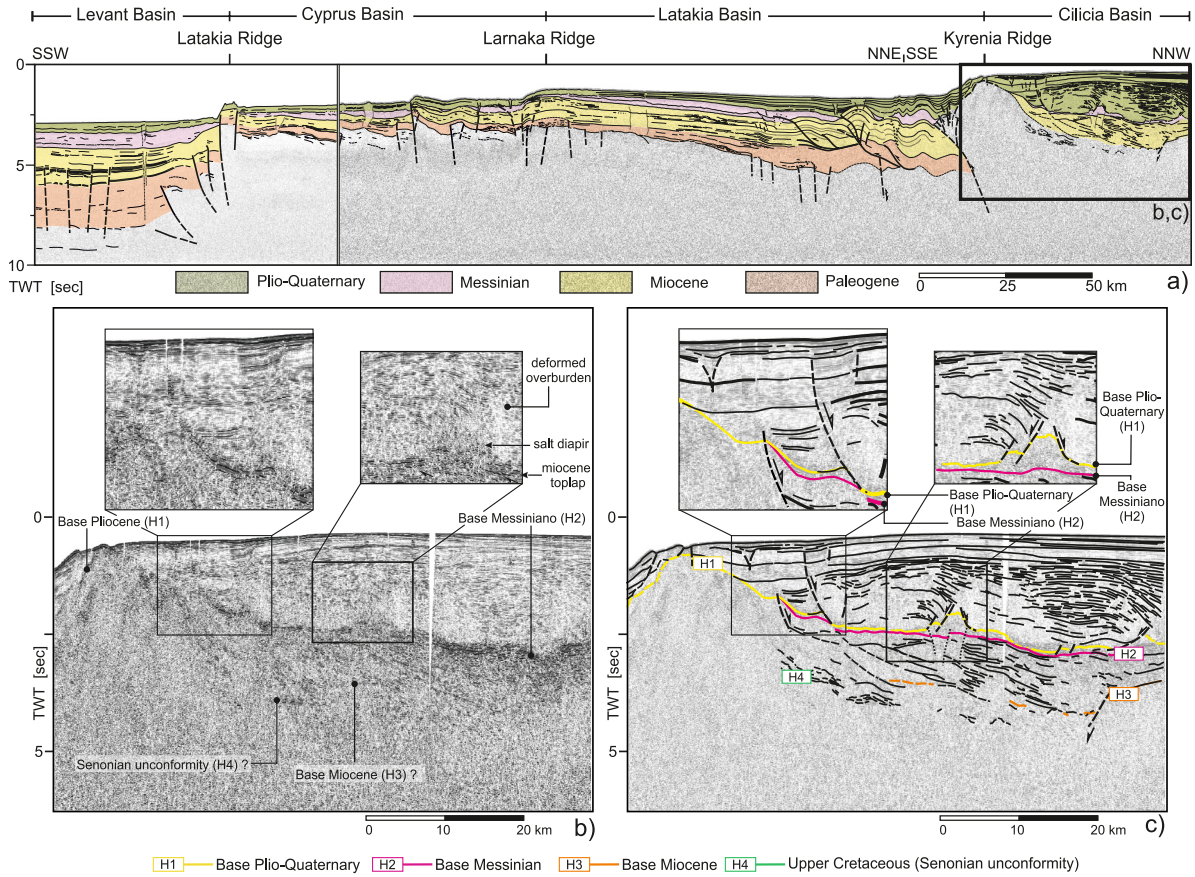

Figure 7. (a) Interpretation and line-drawing overlay on the MS56 TWT seismic section. (b) Zoom of the northernmost part of the seismic section, imaging the northern portion of the Kyrenia Ridge and the Cilicia Basin without the line drawing. (c) Interpreted zoom of the northernmost part of MS56 seismic section imaging the northern portion of the Kyrenia Ridge and the Cilicia Basin.

To build a valid crustal-scale structural model, we integrated our seismic interpretation with the localization along the profile of the boundary between the southward-overthrusting overriding plate (Eurasia–Anatolia) and the northward-underthrusting/subducting plate (Africa) using constraints from Fernández-Blanco et al. (2020) for the central part of the section. In the Latakia Ridge and Levant Basin, we projected the subduction interface into the Triassic evaporites, calibrated by borehole data in the northern Levant Basin (Ghalayini et al., 2018). Here, the evaporites act as a regional detachment level, associated with blind thrusts and folds shaping an accretionary wedge.

Although the basal detachment itself is not imaged directly on the seismic profile, we inferred its geometry from a combination of indirect observations and published models. First, the significant thickness of Paleogene sediments in the Levant Basin and their thinning toward the Latakia Ridge suggest that this zone functioned as a foredeep associated with an active accretionary system. Within this framework, the reverse faults of the southern Latakia Ridge are interpreted as the outer thrusts of an accretionary prism rooted in a deeper detachment.

To support our reconstruction of the subduction interface, we also considered regional geophysical constraints, including gravity modeling (Ergün et al., 2005), seismic refraction data (Feld et al., 2017), and balanced geological cross-sections (Fernández-Blanco et al., 2019). In the inner wedge, where topography dips landward, we assumed an increase in the dip of the basal detachment, in line with the Coulomb critical taper theory (Fuller et al., 2006; Noda, 2016). According to this theory, we assumed that the sum of the topographic slope and the basal dip angle remains constant, meaning a landward-dipping surface requires a steeper basal detachment. We incorporated this adjustment in the transition between the outer and inner wedge (Figure 8c), resulting in a crustal-scale model consistent with the structural architecture of the region.

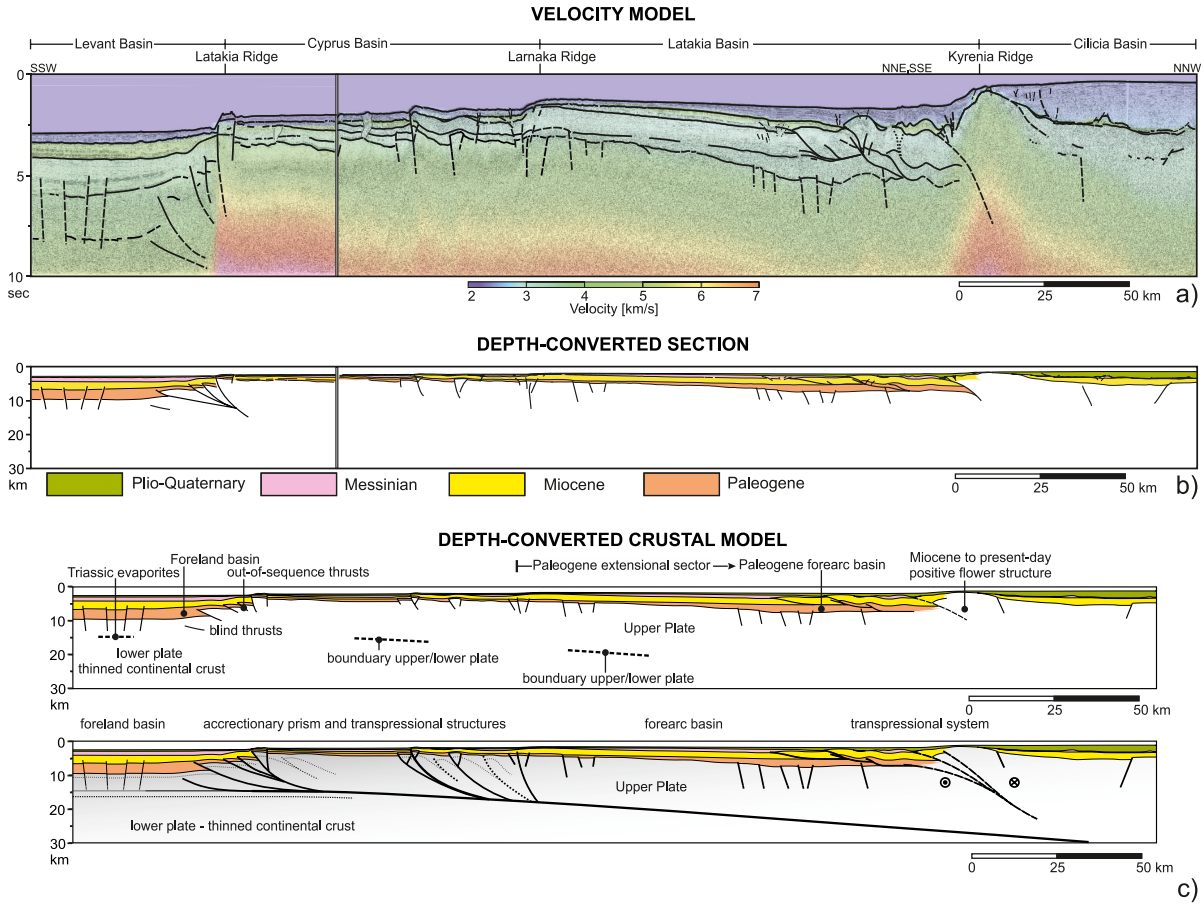

Figure 8. (a) MS56 TWT section with line-drawing of the main reflectors and velocity field used for depth conversion (vertical exaggeration x6). (b) Result from interpreted and depth-converted section. (c) The starting sketch was used to build the crustal model of the lower panel in the upper panel. The location of the boundary between the upper and subducting plate takes advantage of models summarized in Fernández-Blanco et al. (2020).

The final model depicts a subducting plate, composed of thinned continental crust, and an overriding plate, composed of accreted sedimentary and basement units, linked by a mechanically plausible, taper-consistent detachment geometry.

4.4. Tectonic Evolution From the Paleocene to Present-Day

To better describe the tectonic evolution represented in our model, we reconstructed three models corresponding to the end of the Paleocene, Tortonian, and Messinian times (Figure 9). These sections are supported by structural analyses (MOVE software) that allow for the subtraction of deformation along the section plane. Note that this restoration technique has both advantages and limitations in our specific case. For example, one advantage is the precise subtraction of fault offsets, which allows for an admissible result. The limitation is that we cannot consider tectonic movement out-of-plane of our section due to strike-slip movement along the faults. However, a partial application of section balancing techniques provides a valuable solution better than not applying it at all.

Figure 9 shows how the area appeared at the end of the main contractional phase (Figure 9a, end of Paleogene), during the first transpressional phase (Figure 9b, before the Messinian Salinity Crisis) and during the last transpressional phase (Figure 9c, at the end of the Messinian Salinity Crisis).

Starting with the end of the Paleogene sketch, we observe a well-developed accretionary wedge in the southern sector of the overriding plate, characterized by normal faults in the Levant Basin. These faults are related to the flexure of the subducting plate (Africa) under the load of the overriding plate (Eurasia—Anatolia plate). The Cyprus Basin area was affected by compression, which produced the outermost thrust of the Latakia Ridge and out-of-sequence thrusting. These out-of-sequence thrusts are due to a huge volume of sediment deposition in the

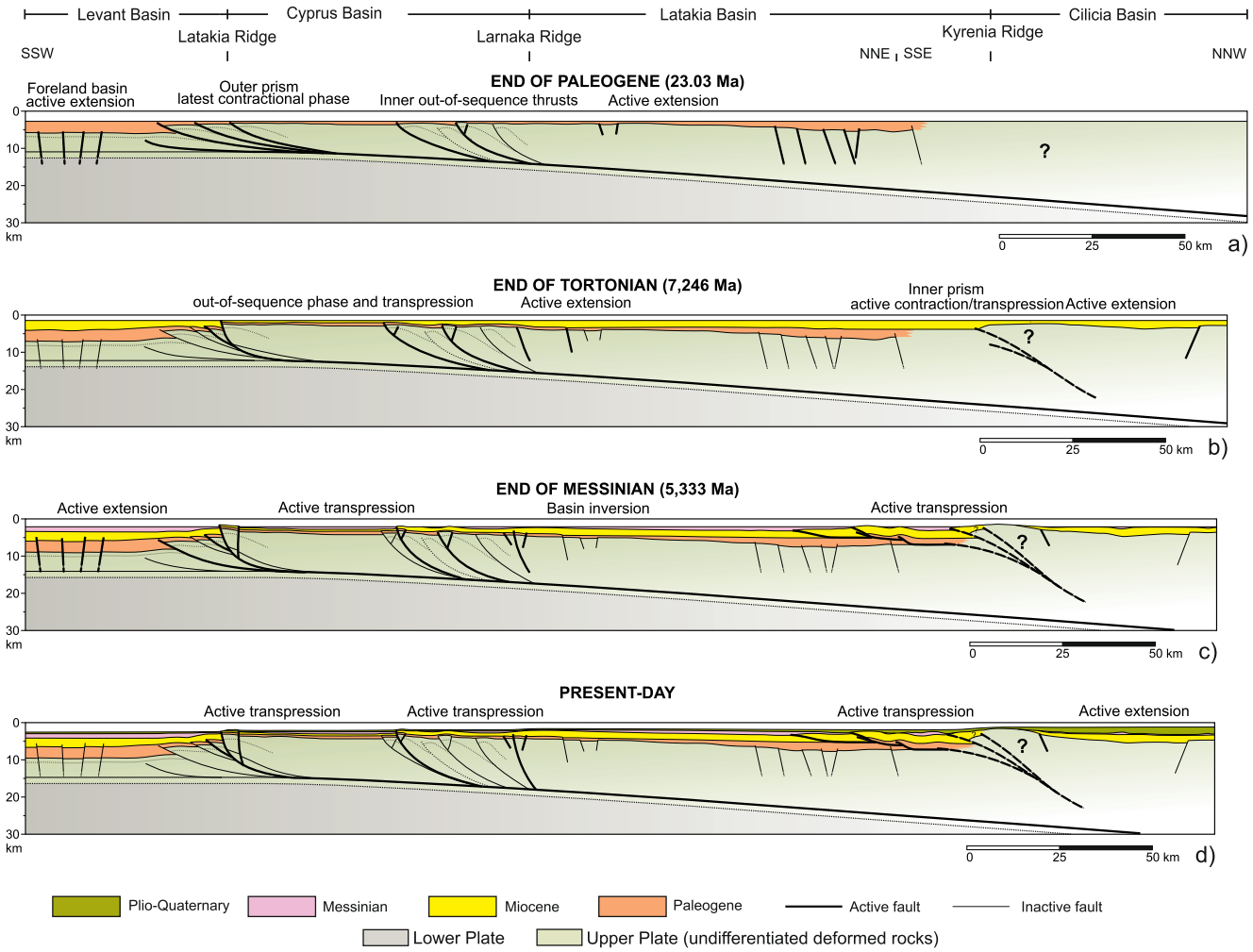

Figure 9. (a) Restored section at the end of the Paleogene (23.03 Ma). (b) Restored section at the end of the Tortonian (7.246 Ma). (c) Restored section at the end of the Messinian (5.333 Ma). (d) Present-day geological section.

foreland. Extensional structures are visible in the Latakia Basin, which represents the forearc basin of the convergent system. We do not have constraints in the Kyrenia Ridge area to provide a viable structure in the Paleogene.

At the end of the Tortonian (Figure 9b), the most external thrust fault of the wedge appeared inactive, and the shortening was accommodated by a few but major out-of-sequence thrusts. This can be explained by (a) the massive thickness of sediments deposited in front of the contractional wedge and (b) the ever-greater thickness of the subducting plate.

At the end of the Messinian (Figure 9c), an oblique reactivation of the main structures began, and normal faulting was active in the Levant Basin. The results were an uplift of the Latakia Ridge, positive tectonic inversion of the Larnaka Ridge, and the development of a thrust system in front of the Kyrenia Ridge. This thrust system was developed mainly in the northern Latakia Basin. Meanwhile, the Cilicia Basin developed as an active extensional basin. Messinian evaporites deposited in local basins separated by structural highs eroded during the rapid sea-level fall of the Messinian salinity crisis. The present-day huge structures, characterized by regional NE-SW alignments, originated from this important transpressive tectonics.

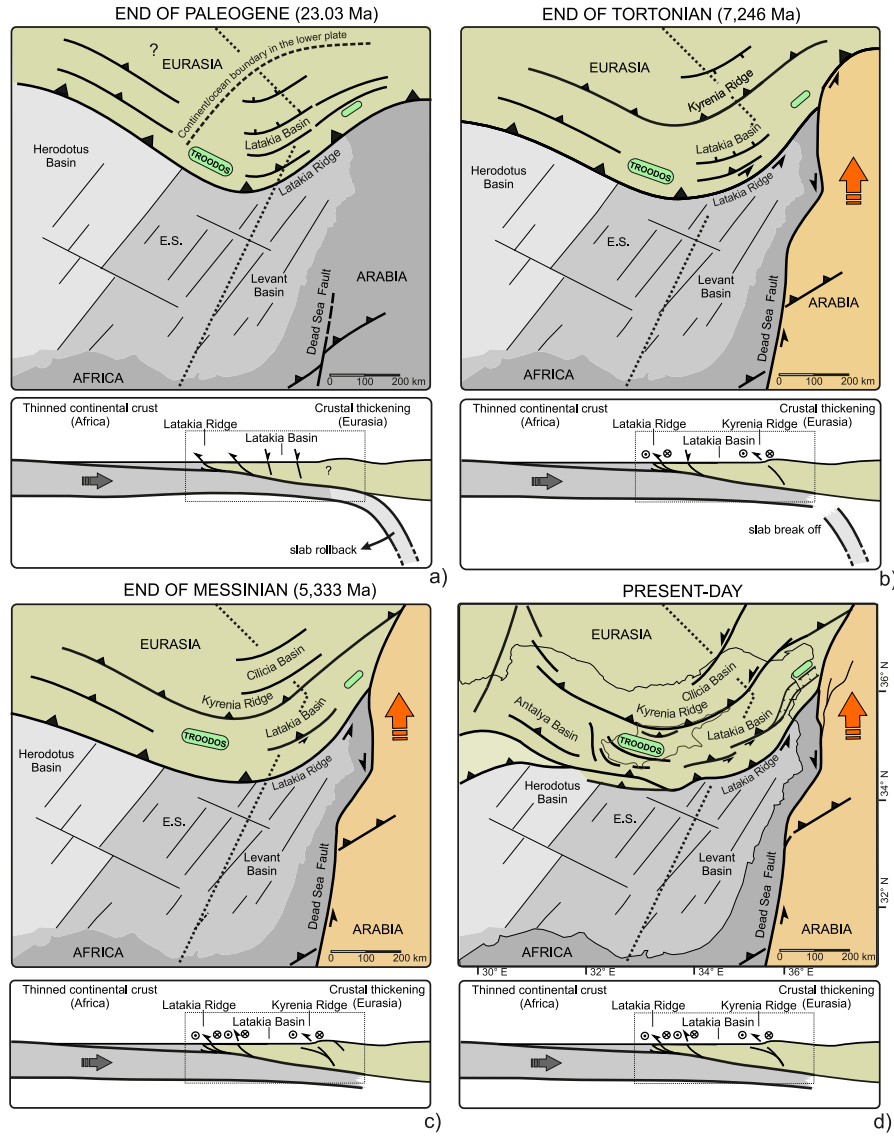

Figure 10. Sketch of the Cenozoic tectonic evolution of the Eastern Mediterranean area. The dotted line indicates the location of our interpreted seismic profile. The green area represents the Eurasian plate; the small light green areas represent the obducted ophiolite. The light gray area represents the oceanic crust of the Herodotus Basin. The gray represents the thinned continental crust of the Levant Basin, while the dark gray area represents the thicker continental crust of the African plate. The orange area represents the Arabian continental crust, undifferentiated in panel. Then, the two plates were divided by the propagation of the Dead Sea Transform Fault. Gray tectonic lineaments are the inherited normal faults of the Tethyan rifting.

5. Discussion

In the previous chapter, we presented a crustal model and a tectonic evolution framework from the Paleogene to the present along a regional profile.

Based on these results, we now integrate our interpretation of the Cenozoic evolution with the major geodynamic events that shaped the eastern Mediterranean region (Figure 10).

Previous studies, such as Hall, Aksu, et al. (2005) and Hall, Calon, et al. (2005), offered valuable early insights into the Latakia–Cyprus system. Their model emphasized out-of-sequence thrusting and transpressional flower structures, inferred from relatively shallow seismic data (~3 s TWT). However, their sections are schematic, unbalanced, and lack temporal constraints or depth conversion. Notably, they interpret structural highs such as the

Larnaka Ridge as long-lived compressional anticlines with ophiolitic cores — essentially static features rooted in basement-involved shortening.

In contrast, our interpretation represents a significant shift. The MS56 profile, with its crustal-scale depth penetration and regional coverage, suggests that the Larnaka Ridge initially formed as part of an extensional zone, likely related to flexural bending of the overriding plate. Evidence includes early normal faults and the shape of sedimentary wedges above. During the Messinian, this zone underwent positive tectonic inversion, with former extensional faults reactivating as reverse faults, leading to uplift. This inversion is dated by angular unconformities and the structure of Messinian evaporites, aligning with the regional shift toward strike-slip-dominated tectonics. This new interpretation of the Larnaka Ridge as an inverted feature, rather than a persistent compressional anticline, is one of the main novel contributions of this study.

More broadly, while Hall, Aksu, et al. (2005) and Hall, Calon, et al. (2005) proposed a two-phase evolution (compressional → transpressional), our model outlines a three-stage tectonic evolution, each supported by kinematic and stratigraphic consistency:

- Paleogene: Development of an accretionary wedge and flexural extension in the Latakia and Levant basins. During this period, the Levant Basin was already acting as the foreland to the south-verging frontal thrust (Figures 9a and 10a). An overfilled accretionary prism developed on the overriding plate in the Latakia Ridge–Cyprus Basin sector (Dickinson, 1995), with the Latakia Ridge frontal thrust consisting of steeply inward-dipping faults. Extensional faulting affected the Latakia Basin, which we interpret as a forearc basin filled with northward-thickening chalk, marls, and turbidites. This forearc extension may be associated with soft frontal collision and slab detachment, triggering retro-wedge deformation. The presence of Upper Cretaceous–Paleogene volcanic rocks in the Kyrenia Range (Chen & Robertson, 2021) suggests the formation of a marginal basin within an oblique convergent setting. In this context, the Kyrenia Ridge could represent a poorly developed volcanic arc, with the Cilicia Basin as its back-arc domain. Although MS56 does not resolve internal reflectors in the Kyrenia Ridge, this hypothesis aligns with our reconstruction. During the Paleogene, the African and Arabian plates gradually separated due to the northward propagation of the Dead Sea Transform Fault (Figure 10), initiating continent–continent soft collision between the Arabian promontory and Eurasia (Agard et al., 2011). This led to the subduction of the thinned Arabian continental margin by the Middle Eocene (Hempton, 1987), which propagated diachronously in both the east and west (Darin & Umhoefer, 2022). While Neotethyan oceanic crust is still being subducted beneath the Makran and the Antalya Basin (Darin & Umhoefer, 2022; Güvercin et al., 2021), the westward thickening of Oligo-Miocene sediments (Bowman, 2011) suggests that, along this profile, the convergence had already slowed by the end of the Paleogene due to the beginning of underthrusting of the attenuated Levant margin. Miocene: The Levant Basin experienced the deposition of a thick, deep-water sedimentary succession, while out-of-sequence thrusting and backthrusting occurred in the outer wedge (Figures 9b and 10b). This deformation style reflects both suture zone thickening during a continued collision (Agard et al., 2011; Darin & Umhoefer, 2022; McPhee & van Hinsbergen, 2019) and the inhibitory effect of thick sediment loads in front of the Latakia Ridge on forward propagation. Concurrently, N-verging normal faults promoted subsidence in the Latakia Basin, allowing the accumulation of thick Miocene turbidites (Harrison, 2008; Harrison et al., 2004; Robertson, 1998a). The coexistence of extensional and compressional domains implies an oblique convergence regime that is already active, with a differentiation between transtensional and transpressional zones (Harrison, 2008) (Figure 10).
- Late Miocene/Messinian: A significant reorganization occurred just before the Messinian Salinity Crisis. The outer wedge continued to deform through out-of-sequence mechanisms, developing into transpressive flower structures, including in the Larnaka Ridge area (Figures 9c and 10c). The forearc basin experienced positive tectonic inversion. At the same time, large amounts of Messinian evaporites were deposited in the deep Levant Basin, in outer wedge minibasins, and more continuously in the Latakia Basin. At the same time, erosional surfaces formed over the main ridges. In front of the Kyrenia Ridge, folding and thrusting occurred before evaporite deposition, as the Messinian units lie in depressions and truncate fold crests. Conversely, the outermost folds show syntectonic growth within evaporites and overlying Plio-Quaternary strata. Since the Messinian, strike-slip deformation has been dominant (Figures 10c and 10d), influenced by the westward escape of the Anatolian microplate and slab rollback in the Hellenic Arc, which helped develop the North and East Anatolian Fault Zones (Schildgen et al., 2014). The Pliocene marine transgression and associated transpression shaped the current configuration (Figures 9d and 10d). Tectonic activity continues today, as

indicated by seafloor folding and faulting around the main ridges and recent growth strata in the Kyrenia Ridge and Cilicia Basin fronts.

In summary, our reconstruction (Figure 9) shows only limited shortening during the Cenozoic, consistent with a convergent margin already shaped by earlier subduction (Ben-Avraham et al., 1995; Biju-Duval & Montadert, 1977; Bowman, 2011; Calon et al., 2005; Hall, Aksu, et al., 2005; Hall, Calon, et al., 2005; Kempler & Garfunkel, 1994; Robertson, 1998a; Symeou et al., 2018; Vidal et al., 2000; Woodside, 1977). The MS56 profile supports a time-calibrated and coherent reconstruction of the eastern Cyprus Arc system, emphasizing the combined effects of oblique convergence, tectonic inversion, and strike-slip partitioning in shaping its Cenozoic development.

6. Conclusion

The MS56 regional seismic profile provides a crustal-scale view of the eastern segment of the Cyprus Arc system, offering new insights into its tectonic evolution from the Paleogene to the present. The depth-converted, structurally admissible interpretation has allowed us to reconstruct a viable geodynamic framework for this region.

Our key conclusions are summarized as follows.

- The eastern margin of the Cyprus Arc underwent a diachronic and partitioned tectonic evolution, characterized by the progressive transition from Paleogene contractional accretion to Messinian and post-Messinian strike-slip deformation with a contractional component. This evolution is summarized in three key tectonic stages, each constrained by stratigraphy and structural geometry.
- Compared to previous literature that regarded the Larnaka Ridge as a compressional anticline, it has now been reinterpreted as a structure that experienced positive tectonic inversion. Originally formed in an extensional setting, the ridge was later reactivated under transpressional conditions, contrary to previous interpretations that considered it as a persistent compressional anticline.
- The deep structure of the margin appears as an interface between a thin continental African plate and an overriding Anatolia–Eurasia plate composed of sedimentary layers, basement fragments, and accreted units. The deformation was accommodated along a regional detachment within Triassic evaporites, consistent with Coulomb wedge theory and supported by borehole calibration and indirect geophysical constraints. The presence of out-of-sequence thrusting, transpressive flower structures, and tectonic inversion features indicates that much of the deformation along the MS56 profile was accommodated obliquely. Strike-slip tectonics became dominant during the Messinian, in line with the regional tectonic reorganization associated with the displacement of the Arabian and Anatolian plates.

This work presents the first consistent crustal model of the eastern Cyprus Arc system, providing a solid framework for understanding how oblique convergence and tectonic inheritance have influenced one of the most structurally complex regions of the Eastern Mediterranean.

Conflict of Interest

The authors declare no conflicts of interest relevant to this study.

Data Availability Statement

This manuscript does not include any new data.

Acknowledgments
We sincerely thank the Editor, Federico Rossetti, the Associate Editor, and reviewers David Iacopini and Amir Joffe for their constructive feedback, which significantly improved this manuscript. We also acknowledge the use of Petex Move and Schlumberger Petrel, provided under academic license agreements, for structural, seismic, and geological modeling. Open access publishing facilitated by Universita degli Studi di Trieste, as part of the Wiley - CRUI-CARE agreement.

References

Agard, P., Omrani, J., Jolivet, L., Whitechurch, H., Vrielynck, B., Spakman, W., et al. (2011). Zagros orogeny: A subduction-dominated process. *Geological Magazine*, *148*(5–6), 692–725. https://doi.org/10.1017/s001675681100046x

Aksu, A. E., Hall, J., & Yaltırak, C. (2021). Miocene–quaternary tectonic, kinematic and sedimentary evolution of the eastern Mediterranean Sea: A regional synthesis. *Earth-Science Reviews*, *220*, 103719. https://doi.org/10.1016/j.earscirev.2021.103719

Alsouki, M., Alali, N., & Alattabi, A. N. (2019). The seismic evidence of passively evolving Messinian salt in offshore Syria. In *Journal of physics: Conference series* (Vol. 1279). IOP Publishing, 012042.

Ben-Avraham, Z., Tibor, G., Limonov, A. F., Leybov, M. B., Ivanov, M. K., Tokarev, M. Y., & Woodside, J. M. (1995). Structure and tectonics of the eastern Cyprean Arc. *Marine and Petroleum Geology*, *12*(3), 263–271. https://doi.org/10.1016/0264-8172(95)98379-j

Biju-Duval, B., & Montadert, L. (1977). Introduction to the structural history of the Mediterranean basins. In *Structural history of the Mediterranean Basins* (pp. 1–12). Technip Paris.

Bilim, F., Aydemir, A., & Ates, A. (2017). Tectonics and thermal structure in the Gulf of Iskenderun (southern Turkey) from the aeromagnetic, borehole and seismic data. *Geothermics*, *70*, 206–221. https://doi.org/10.1016/j.geothermics.2017.06.016

Bowman, S. A. (2011). Regional seismic interpretation of the hydrocarbon prospectivity of offshore Syria. *GeoArabia*, *16*(3), 95–124. https://doi.org/10.2113/geoarabia160395

Bragin, N., Bragina, L., Tsiolakis, E., & Symeou, V. (2021). The Upper Cretaceous Mamonia Mélange (Petra tou Romiou, southwestern Cyprus): Composition and age. *Cretaceous Research*, *125*, 104850. https://doi.org/10.1016/j.cretres.2021.104850

Brancatelli, G., Forlin, E., Bertone, N., Del Ben, A., & Geletti, R. (2022). Time to depth seismic reprocessing of vintage data: A case study in the Otranto channel (South Adriatic Sea). In *Interpreting subsurface seismic data* (pp. 157–197). Elsevier.

Calon, T. J., Aksu, A. E., & Hall, J. (2005). The Neogene evolution of the outer Latakia Basin and its extension into the eastern Mesaoria Basin (Cyprus), eastern Mediterranean. *Marine Geology*, *221*(1–4), 61–94. https://doi.org/10.1016/j.margeo.2005.03.013

Camerlenghi, A., Del Ben, A., Hübscher, C., Forlin, E., Geletti, R., Brancatelli, G., et al. (2019). Seismic markers of the Messinian salinity crisis in the deep Ionian Basin. *Basin Research*, *32*(4), 716–738. https://doi.org/10.1111/bre.12392

Chen, G., & Robertson, A. H. (2021). Evidence from late Cretaceous-Paleogene volcanic rocks of the Kyrenia Range, Northern Cyprus for the northern, active continental margin of the southern Neotethys. *Lithos*, *380*, 105835. https://doi.org/10.1016/j.lithos.2020.105835

Çiftçí, S. Y., Haciköylü, P., Geze Kalanyuva, Y., Kansu, E., & Aktepe, A. (2012). Exploration plays in the Mersin Basin, Turkish Mediterranean Sea. *The Leading Edge*, *31*(7), 832–845. https://doi.org/10.1190/tle31070832.1

Civile, D., Brancolini, G., Lodolo, E., Forlin, E., Accaino, F., Zecchin, M., et al. (2021). Morphostructural setting and tectonic evolution of the central part of the Sicilian channel (Central Mediterranean). *Lithosphere*, *2021*(1), 7866771. https://doi.org/10.2113/2021/7866771

Darin, M. H., & Umhoefer, P. J. (2022). Diachronous initiation of Arabia–Eurasia collision from eastern Anatolia to the southeastern Zagros Mountains since middle Eocene time. *International Geology Review*, *64*(18), 1–29. https://doi.org/10.1080/00206814.2022.2048272

Dickinson, W. R. (1995). Forearc basins. Tectonics of sedimentary basins (pp. 221–261).

Dilek, Y., & Robinson, P. T. (2003). *Ophiolites in Earth history: Introduction* (Vol. 218(1), 1–8). Geological Society, London, Special Publications. https://doi.org/10.1144/gsl.sp.2003.218.01.01

Druckman, Y., Buchbinder, B., Martinotti, G. M., Tov, R. S., & Aharon, P. (1995). The buried Afiq Canyon (eastern Mediterranean, Israel): A case study of a Tertiary submarine canyon exposed in late Messinian times. *Marine Geology*, *123*(3–4), 167–185. https://doi.org/10.1016/0025-3227(94)00127-7

Ergün, M., Okay, S., Sari, C., Oral, E. Z., Ash, M., Hall, J., & Miller, H. (2005). Gravity anomalies of the Cyprus Arc and their tectonic implications. *Marine Geology*, *221*(1–4), 349–358. https://doi.org/10.1016/j.margeo.2005.03.004

Faccenna, C., Bellier, O., Martinod, J., Piromallo, C., & Regard, V. (2006). Slab detachment beneath eastern Anatolia: A possible cause for the formation of the North Anatolian fault. *Earth and Planetary Science Letters*, *242*(1–2), 85–97. https://doi.org/10.1016/j.epsl.2005.11.046

Feld, C., Mechie, J., Hübscher, C., Hall, J., Nicolaides, S., Gurbuz, C., et al. (2017). Crustal structure of the Eratosthenes Seamount, Cyprus and S. Turkey from an amphibian wide-angle seismic profile. *Tectonophysics*, *700*, 32–59.

Feng, Y. E., Yankelzon, A., Steinberg, J., & Reshef, M. (2016). Lithology and characteristics of the Messinian evaporite sequence of the deep levant Basin, eastern Mediterranean. *Marine Geology*, *376*, 118–131. https://doi.org/10.1016/j.margeo.2016.04.004

Fernández-Blanco, D., Bertotti, G., Aksu, A., & Hall, J. (2019). Monoclinal flexure of an orogenic plateau margin during subduction, south Turkey. *Basin Research*, *31*(4), 709–727. https://doi.org/10.1111/bre.12341

Fernández-Blanco, D., Mannu, U., Bertotti, G., & Willett, S. D. (2020). Forearc high uplift by lower crustal flow during growth of the Cyprus-Anatolian margin. *Earth and Planetary Science Letters*, *544*, 116314. https://doi.org/10.1016/j.epsl.2020.116314

Festa, A., Pini, G. A., Dilek, Y., & Codegone, G. (2010). Mélanges and mélange-forming processes: A historical overview and new concepts. *International Geology Review*, *52*(10–12), 1040–1105. https://doi.org/10.1080/00206810903557704

Finetti, I., & Morelli, C. (1973). Geophysical exploration of the Mediterranean Sea.

Follows, E. J. (1992). Patterns of reef sedimentation and diagenesis in the Miocene of Cyprus. *Sedimentary Geology*, *79*, 225–253. https://doi.org/10.1016/0037-0738(92)90013-H

Frizon de Lamotte, D., Raulin, C., Mouchot, N., Wrobel-Daveau, J. C., Blanpied, C., & Ringenbach, J. C. (2011). The southernmost margin of the Tethys realm during the Mesozoic and Cenozoic: Initial geometry and timing of the inversion processes. *Tectonics*, *30*(3). https://doi.org/10.1029/2010tc002691

Fuller, C. W., Willett, S. D., & Brandon, M. T. (2006). Formation of forearc basins and their influence on subduction zone earthquakes. *Geology*, *34*(2), 65–68. https://doi.org/10.1130/g21828.1

Gao, H., Tong, X., Wen, Z., & Wang, Z. (2019). The tectonic evolution of the eastern Mediterranean basin and its control on hydrocarbon distribution. *Journal of Petroleum Science and Engineering*, *178*, 389–407. https://doi.org/10.1016/j.petrol.2019.03.029

Gardosh, M., Druckman, Y., Buchbinder, B., & Rybakov, M. (2008). *The levant Basin offshore Israel: Stratigraphy, structure, tectonic evolution and implications for hydrocarbon exploration* (p. 119). Geophysical Institute of Israel

Gardosh, M. A., & Druckman, Y. (2006). Seismic stratigraphy, structure and tectonic evolution of the Levantine Basin, offshore Israel. In A. H. F. Robertson, & D. Mountrakis (Eds.), *Tectonic' Development of the Eastern Mediterranean Region* (Vol. 260, pp. 201–227). Geological Society, London, Special Publications. https://doi.org/10.1144/gsl.sp.2006.260.01.09

Gardosh, M. A., Garfunkel, Z., Druckman, Y., & Buchbinder, B. (2010). *Tethyan rifting in the Levant Region and its role in early Mesozoic crustal evolution* (Vol. 341, pp. 9–36). Geological Society, London, Special Publications. https://doi.org/10.1144/sp341.2

Garfunkel, Z. (2004). Origin of the Eastern Mediterranean basin: A reevaluation. *Tectonophysics*, *391*(1–4), 11–34. https://doi.org/10.1016/j.tecto.2004.07.006

GeoMapApp. (n.d.). Retrieved from http://www.geomapapp.org

Ghalayini, R., Daniel, J. M., Homberg, C., Nader, F. H., & Comstock, J. E. (2014). Impact of Cenozoic strike-slip tectonics on the evolution of the northern Levant Basin (offshore Lebanon). *Tectonics*, *33*(11), 2121–2142. https://doi.org/10.1002/2014tc003574

Ghalayini, R., Nader, F. H., Bou Daher, S., Hawie, N., & Chbat, W. E. (2018). Petroleum systems of Lebanon: An update and review. *Journal of Petroleum Geology*, *41*(2), 189–214. https://doi.org/10.1111/jpg.12700

Granot, R. (2016). Palaeozoic oceanic crust preserved beneath the eastern Mediterranean. *Nature Geoscience*, *9*(9), 701–705. https://doi.org/10.1038/ngeo2784

Güvercin, S. E., Konca, A. Ö., Özbakır, A. D., Ergintav, S., & Karabulut, H. (2021). New focal mechanisms reveal fragmentation and active subduction of the Antalya slab in the Eastern Mediterranean. *Tectonophysics*, *805*, 228792. https://doi.org/10.1016/j.tecto.2021.228792

Gvirtzman, Z., Manzi, V., Calvo, R., Gavrieli, I., Gennari, R., Lugli, S., et al. (2017). Intra-Messinian truncation surface in the Levant Basin explained by subaqueous dissolution. *Geology*, *45*(10), 915–918. https://doi.org/10.1130/g39113.1

Hall, J., Aksu, A. E., Calon, T. J., & Yaşar, D. (2005). Varying tectonic control on basin development at an active microplate margin: Latakia Basin, Eastern Mediterranean. *Marine Geology*, *221*(1–4), 15–60. https://doi.org/10.1016/j.margeo.2004.05.034

Hall, J., Calon, T. J., Aksu, A. E., & Meade, S. R. (2005). Structural evolution of the Latakia Ridge and Cyprus Basin at the front of the Cyprus Arc, eastern Mediterranean Sea. *Marine Geology*, *221*(1–4), 261–297. https://doi.org/10.1016/j.margeo.2005.03.007

Harrison, R. W. (2008). A model for the plate tectonic evolution of the eastern Mediterranean region that emphasizes the role of transform (strike-slip) structures. In *1st WSEAS international conference on environmental and geological science and engineering (EG'08) Malta*.

Harrison, R. W., Newell, W. L., Batıhanlı, H., Panayides, I., McGeehin, J. P., Mahan, S. A., et al. (2004). Tectonic framework and late Cenozoic tectonic history of the northern part of Cyprus: Implications for earthquake hazards and regional tectonics. *Journal of Asian Earth Sciences*, *23*(2), 191–210. https://doi.org/10.1016/s1367-9120(03)00095-6

Hawie, N., Gorini, C., Deschamps, R., Nader, F. H., Montadert, L., Granjeon, D., & Baudin, F. (2013). Tectono-stratigraphic evolution of the northern Levant Basin (offshore Lebanon). *Marine and Petroleum Geology*, *48*, 392–410. https://doi.org/10.1016/j.marpetgeo.2013.08.004

Hempton, M. R. (1987). Constraints on Arabian plate motion and extensional history of the Red Sea. *Tectonics*, *6*(6), 687–705. https://doi.org/10.1029/tc006i006p00687

Kempler, D., & Garfunkel, Z. (1994). Structures and kinematics in the northeastern Mediterranean: A study of an irregular plate boundary. *Tectonophysics*, *234*(1–2), 19–32. https://doi.org/10.1016/0040-1951(94)90202-x

Khair, K., & Tsokas, G. N. (1999). Nature of the Levantine (eastern Mediterranean) crust from multiple-source Werner deconvolution of Bouguer gravity anomalies. *Journal of Geophysical Research*, *104*(B11), 25469–25478. https://doi.org/10.1029/1999jb900228

Kinnaird, T., & Robertson, A. (2013). *Tectonic and sedimentary response to subduction and incipient continental collision in southern Cyprus, easternmost Mediterranean region* (Vol. 372, pp. 585–614). Geological Society. https://doi.org/10.1144/sp372.10

Klaeschen, D., Vidal, N., Kopf, A. J., von Huene, R., & Krasheninnikov, V. A. (2005). Multi-channel seismic profiles across Eratosthenes seamount and the florence rise reflecting the incipient collision between Africa and Eurasia near the island of Cyprus, eastern Mediterranean.

Lapierre, H., Bosch, D., Narros, A., Mascle, G. H., Tardy, M., & Demant, A. (2007). The Mamonia complex (SW Cyprus) revisited: Remnant of Late Triassic intra-oceanic volcanism along the Tethyan southwestern passive margin. *Geological Magazine*, *144*(1), 1–19. https://doi.org/10.1017/s0016756806002937

Longacre, M., Bentham, P., Hanbal, I., Cotton, J., & Edwards, R. (2007). New crustal structure of the Eastern Mediterranean basin: Detailed integration and modeling of gravity, magnetic, seismic refraction, and seismic reflection data. In *EGM 2007 International workshop* (p. cp-166). European Association of Geoscientists & Engineers

Maffione, M., van Hinsbergen, D. J., de Gelder, G. I., van der Goes, F. C., & Morris, A. (2017). Kinematics of Late Cretaceous subduction initiation in the Neo-Tethys ocean reconstructed from ophiolites of Turkey, Cyprus, and Syria. *Journal of Geophysical Research: Solid Earth*, *122*(5), 3953–3976. https://doi.org/10.1002/2016jb013821

Maillard, A., Hübscher, C., Benkhelil, J., & Tahchi, E. (2011). Deformed Messinian markers in the Cyprus Arc: Tectonic and/or Messinian salinity crisis indicators? *Basin Research*, *23*(2), 146–170. https://doi.org/10.1111/j.1365-2117.2010.00464.x

Malpas, J., Xenophontos, C., & Williams, D. (1992). The Ayia Varvara formation of SW Cyprus: A product of complex collisional tectonics. *Tectonophysics*, *212*(3–4), 193–211. https://doi.org/10.1016/0040-1951(92)90291-d

Mart, Y., & Robertson, A. H. F. (1998). Eratosthenes seamount: An oceanographic yardstick recording the late Mesozoic–Tertiary geological history of the Eastern Mediterranean. In A. H. F. Robertson, K.-C. Emeis, C. Richter, & A. Camerlenghi (Eds.), *Proceedings of the ocean drilling program, scientific results* (Vol. 160, pp. 701–708).

McCay, G. A., & Robertson, A. H. F. (2013). *Upper Miocene–Pleistocene deformation of the Girne (Kyrenia) range and dar Dere (Ovgos) lineaments, Northern Cyprus: Role in collision and tectonic escape in the easternmost Mediterranean region* (Vol. 372(1), pp. 421–445). Geological Society, London, Special Publications. https://doi.org/10.1144/sp372.6

McClusky, S., Balassanian, S., Barka, A., Demir, C., Ergintav, S., Georgiev, I., et al. (2000). Global positioning system constraints on plate kinematics and dynamics in the eastern Mediterranean and Caucasus. *Journal of Geophysical Research*, *105*(B3), 5695–5719. https://doi.org/10.1029/1999jb900351

McPhee, P. J., & van Hinsbergen, D. J. (2019). Tectonic reconstruction of Cyprus reveals late Miocene continental collision of Africa and Anatolia. *Gondwana Research*, *68*, 158–173. https://doi.org/10.1016/j.gr.2018.10.015

Miyashiro, A. (1974). Volcanic rock series in island arcs and active continental margins. *American Journal of Science*, *274*(4), 321–355. https://doi.org/10.2475/ajs.274.4.321

Moix, P., Kozur, H. W., Stampfli, G. M., Mostler, H., Lucas, S. G., & Spielmann, J. A. (2007). New paleontological, biostratigraphical and paleogeographic results from the Triassic of the Mersin Mélange, SE Turkey. *The Global Triassic. New Mexico Museum of Natural History Science Bulletin*, *41*, 282–311.

Montadert, L., Nicolaides, S., Semb, P. H., & Lie, Ø. (2014). Petroleum systems offshore Cyprus.

Moores, E. M., & Vine, F. J. (1971). The Troodos Massif, Cyprus and other ophiolites as oceanic crust: Evaluation and implications. *Philosophical Transactions of the Royal Society of London,Series A*, *268*(1192), 443–467.

Morris, A., Anderson, M. W., Inwood, J., & Robertson, A. H. (2006). *Palaeomagnetic insights into the evolution of Neotethyan oceanic crust in the eastern Mediterranean* (Vol. 260, pp. 351–372). Geological Society, London, Special Publications. https://doi.org/10.1144/gsl.sp.2006.260.01.15

Nader, F. H., Inati, L., Ghalayini, R., Hawie, N., & Daher, S. B. (2018). Key geological characteristics of the Saida-Tyr platform along the eastern margin of the levant basin, offshore Lebanon: Implications for hydrocarbon exploration. *Oil & Gas Science and Technology–Revue d'IFP Energies Nouvelles*, *73*, 50. https://doi.org/10.2516/ogst/2018045

Netzeband, G. L., Gohl, K., Hübscher, C. P., Ben-Avraham, Z., Dehghani, G. A., Gajewski, D., & Liersch, P. (2006). The Levantine Basin—Crustal structure and origin. *Tectonophysics*, *418*(3–4), 167–188. https://doi.org/10.1016/j.tecto.2006.01.001

Noda, A. (2016). Forearc basins: Types, geometries, and relationships to subduction zone dynamics. *Bulletin*, *128*(5–6), 879–895. https://doi.org/10.1130/b31345.1

Papadimitriou, N., Gorini, C., Nader, F. H., Deschamps, R., Symeou, V., & Lecomte, J. C. (2018). Tectono-stratigraphic evolution of the western margin of the Levant Basin (offshore Cyprus). *Marine and Petroleum Geology*, *91*, 683–705. https://doi.org/10.1016/j.marpetgeo.2018.02.006

Pearce, J. A. (2003). Supra-subduction zone ophiolites: The search for modern analogues. In Y. Dilek & S. Newcomb (Eds.), *Ophiolite concept and the evolution of geological thought* (Vol. 373, pp. 269–293). Geological Society of America Special Paper. https://doi.org/10.1130/0-8137-2373-6.269

Pearce, J. A., & Robinson, P. T. (2010). The troodos ophiolitic complex probably formed in a subduction initiation, slab edge setting. *Gondwana Research*, *18*(1), 60–81. https://doi.org/10.1016/j.gr.2009.12.003

Ring, U., & Pantazides, H. (2019). The uplift of the Troodos massif, Cyprus. *Tectonics*, *38*(8), 3124–3139. https://doi.org/10.1029/2019tc005514

Robertson, A. H. (1998a). Mesozoic-Tertiary tectonic evolution of the easternmost Mediterranean area: Integration of marine and land evidence. *Proceedings of the Ocean Drilling Program, Scientific Results*, *160*. Chapter 54.

Robertson, A. H., Parlak, O., & Ustaömer, T. (2012). Overview of the Palaeozoic–Neogene evolution of neotethys in the Eastern Mediterranean region (southern Turkey, Cyprus, Syria). *Petroleum Geoscience*, *18*(4), 381–404. https://doi.org/10.1144/petgeo2011-091

Robertson, A. H. F. (1998b). Tectonic significance of the Eratosthenes seamount: A continental fragment in the process of collision with a subduction zone in the eastern Mediterranean (Ocean drilling program leg 160). *Tectonophysics*, *298*(1–3), 63–82. https://doi.org/10.1016/s0040-1951(98)00178-4

Robertson, A. H. F., & Kinnaird, T. C. (2016). Structural development of the central Kyrenia Range (North Cyprus) in its regional setting in the eastern Mediterranean region. *International Journal of Earth Sciences*, *105*(1), 417–437. https://doi.org/10.1007/s00531-015-1215-x

Robertson, A. H. F., & Woodcock, N. H. (1979). Mamonia complex, Southwest Cyprus: Evolution and emplacement of a Mesozoic continental margin. *Bulletin of the Geological Society of America*, *90*(7), 651–665. https://doi.org/10.1130/0016-7606(1979)90<651:mcscea>2.0.co;2

Rybakov, M., Goldshmidt, V., Hall, J. K., Ben-Avraham, Z., & Lazar, M. (2011). New insights into the sources of magnetic anomalies in the levant. *Russian Geology and Geophysics*, *52*(4), 377–397. https://doi.org/10.1016/j.rgg.2011.03.001

Sampietro, D., Mansi, A. H., & Capponi, M. (2018). Moho depth and crustal architecture beneath the Levant Basin from global gravity field model. *Geosciences*, *8*(6), 200. https://doi.org/10.3390/geosciences8060200

Schattner, U., & Ben-Avraham, Z. (2007). Transform margin of the northern Levant, eastern Mediterranean: From formation to reactivation. *Tectonics*, *26*(5). https://doi.org/10.1029/2007tc002112

Schildgen, T. F., Yıldırım, C., Cosentino, D., & Strecker, M. R. (2014). Linking slab break-off, Hellenic trench retreat, and uplift of the Central and Eastern Anatolian plateaus. *Earth-Science Reviews*, *128*, 147–168. https://doi.org/10.1016/j.earscirev.2013.11.006

Segev, A., Sass, E., & Schattner, U. (2018). Age and structure of the Levant basin, Eastern Mediterranean. *Earth-Science Reviews*, *182*, 233–250. https://doi.org/10.1016/j.earscirev.2018.05.011

Smaily, L. I. (2017). *Lithosphere dynamics and architecture of the levant basin margins: Integrated geophysical approach*. Doctoral dissertation. Université Pierre et Marie Curie-Paris VI; Université Saint-Joseph (Beyrouth). Ecole supérieure d'ingénieurs de Beyrouth.

Steinberg, J., Roberts, A. M., Kusnir, N. J., Schafer, K., & Karcz, Z. (2018). Crustal structure and post-rift evolution of the Levant Basin. *Marine and Petroleum Geology*, *96*, 522–543. https://doi.org/10.1016/j.marpetgeo.2018.05.006

Symeou, V., Homberg, C., Nader, F. H., Darnault, R., Lecomte, J. C., & Papadimitriou, N. (2018). Longitudinal and temporal evolution of the tectonic style along the Cyprus Arc system, assessed through 2-D reflection seismic interpretation. *Tectonics*, *37*(1), 30–47. https://doi.org/10.1002/2017tc004667

Taylor, R. N., Ishizuka, O., Hessey, I., Michalik, A., Stillwell, L., & White, S. (2022). Isotope track Tethyan seamount subduction beneath the Troodos spreading center, Cyprus. *Earth and Planetary Science Letters*, *584*, 117509. https://doi.org/10.1016/j.epsl.2022.117509

Van Hinsbergen, D. J., Torsvik, T. H., Schmid, S. M., Maţenco, L. C., Maffione, M., Vissers, R. L., et al. (2020). Orogenic architecture of the Mediterranean region and kinematic reconstruction of its tectonic evolution since the Triassic. *Gondwana Research*, *81*, 79–229. https://doi.org/10.1016/j.gr.2019.07.009

Verschuur, D. J., Berkhout, A. J., & Wapenaar, C. P. A. (1992). Adaptive surface-related multiple elimination. *Geophysics*, *57*(9), 1166–1177. https://doi.org/10.1190/1.1443330

Vidal, N., Alvarez-Marrón, J., & Klaeschen, D. (2000). The structure of the Africa-Anatolia plate boundary in the eastern Mediterranean. *Tectonics*, *19*(4), 723–739. https://doi.org/10.1029/2000tc900011

Welford, K., Hall, J., Huebscher, C., Reiche, S., & Louden, K. (2015). Crustal seismic velocity structure from eratosthenes seamount to hecataeus rise across the Cyprus Arc, eastern Mediterranean. *Geophysical Journal International*, *200*, 935–953.

Wiggins, J. W. (1988). Attenuation of complex water-bottom multiples by wave-equation-based prediction and subtraction. *Geophysics*, *53*(12), 1527–1539. https://doi.org/10.1190/1.1442434

Woodside, J. M. (1977). Tectonic elements and crust of the eastern Mediterranean Sea. *Marine Geophysical Researches*, *3*(3), 317–354. https://doi.org/10.1007/bf00285658